ECMWF COPERNICUS REPORT

Copernicus Climate Change Service

A scientific assessment of the usability of the RCP-GCM-RCM setup

D34b_Lot2.1.4.2

Issued by: SMHI/ Anna Eronn

Date: 11/7/2021

Ref: C3S_D34b_Lot2.1.4.2_A scientific assessment of the usability of the RCP-GCM-RCM setup _v4

Contributors

DMI
Ole B. Christensen
Fredrik Boberg

SMHI
Grigory Nikulin
Erik Kjellström

ETHZ
Marie-Estelle Demory
Jan Rajczak
Christoph Schär

CNRS
Robert Vautard

MF
Samuel Somot
Lola Corre

ICTP
Erika Coppola

OGS
James Ciarlo
Cosimo Solidoro

MOHC
Erasmo Buonomo
Richard Jones

HZG
Claas Teichmann

Katharina Bülow

KNMI
Erik van Meijgaard

Table of Contents

Executive Summary

This report is the final Work Package 1 deliverable D34b_Lot2.1.4.2 of the COPERNICUS C3S_D34b_Lot2 (PRINCIPLES) project. It outlines a scientific assessment of the usability of the experimental setup for the choice of forcing scenarios (RCPs), global (GCMs) and regional climate models (RCMs), which has been followed in C3S_34b_Lot2 (PRINCIPLES). The project has made considerable progress towards filling a matrix of downscaled CMIP5 global simulations for 3 RCP emission scenarios, 8 GCMs, and 11 RCMs. For computational reasons, it is not possible to complete the matrix. Instead, PRINCIPLES has focused on combining RCP-GCM-RCM building blocks in a rational and efficient way. As the matrix is not completely filled, it is important to evaluate the choice of the strategy and to investigate to which extent the partly filled matrix resembles a hypothetical full matrix. This evaluation may be used as guidance for the design of future similar exercises including, for instance, CMIP6 GCMs.

At the end of the PRINCIPLES project, a considerable expansion of the EURO-CORDEX RCPxGCMxRCM matrix has been performed. Following the plan laid out in Deliverable D34b_Lot2.1.4.1, this report presents an analysis of the robustness of the existing ensemble results through two independent analyses: 1) a comparison between properties of the current RCP8.5 GCMxRCM matrix with an emulated complete matrix using the ANOVA-based procedure laid out in D1.4.1 and in Christensen and Kjellström (2021); 2) an investigation of the effect of the many added simulations compared to the situation before PRINCIPLES on the EUR-11 ensemble median and spread of the climate change signal under the RCP8.5 scenario.

The first part of this report outlines the feasibility and effect of filling the matrix as described in the planning deliverable D34b_Lot2.1.4.1. Missing simulations have been emulated with an analysis-of-variance (ANOVA) based technique in order to obtain 8x11 GCMxRCM matrices of seasonal average climatological fields and their associated climate change. In this analysis, we study 30-year averages of seasonal-mean surface air temperature, precipitation amount and average 10m wind speed, and concentrate on climate change between two such periods and the RCP8.5 scenario. The method works well in situations where a large part of the total ensemble variability is determined by the GCM and/or RCM choice; it is not useful in cases where interannual variability dominates, like extremes and other fields with a large internal variability.

The ANOVA-based technique gives large relative improvements of ensemble averages for all fields considered, but the improvements are still small compared to the geographical variation of climate change and can be replaced by direct ensemble averages without large differences in results, due to the high degree of filling already present in the current matrix. Consequently, for more sparsely filled matrices the improvement can potentially be larger although we note that there is a lower limit to which the matrix needs to be filled in order for the technique to work. A quantitative analysis of the effect of filling on types of ensemble averaging can be found in Christensen and Kjellström (2021).

In the second part of the report, we assess the effect of the additional PRINCIPLES simulations in the climate change signal projected by the GCM-RCM matrix under the RCP8.5 scenario. We concentrate on mean values of air temperature at 2 m and precipitation as well as precipitation extremes, and base our analyses on Rajczak and Schär (2017). Our results show that the additional PRINCIPLES simulations increase our confidence in mean temperature and mean and extreme precipitation projected by the current generation of EUR-11 regional climate models. The new simulations make the ensemble median slightly colder and wetter, especially in summer, than the small EUR-11 ensemble already available before the start of PRINCIPLES. Most additional simulations tend to also be closer to each other, which decreases the ensemble interquartile range. However, adding new GCM-RCM simulations tends to slightly increase the ensemble spread, which varies depending on regions and seasons. The large EUR-11 ensemble therefore offers a unique opportunity to understand the drivers of the climate change signals projected by EUR-11 GCM-RCM simulations.

The two studies outlined below are still ongoing. Further analyses will be performed and published after the end of the present contract.

1. Completing the GCMxRCM matrix with emulated values

1.1 Introduction

Building on the planning deliverable D34b_Lot2.1.4.1, missing simulations have been emulated with an analysis-of-variance (ANOVA) based technique in order to obtain 8x11 GCMxRCM matrices of seasonal average climatological fields and their associated climate change.

The study aims to "fill" the 3-dimensional (RCP x GCM x RCM) matrix of EURO-CORDEX simulations that existed at the onset of the project as far as possible. The main question, which should be addressed, is whether the current EURO-CORDEX ensemble after PRINCIPLES is "big enough" to be trustworthy. This should be put as a quantitative question, and a technique has been devised during the project, where a full matrix is emulated from the partly filled matrix. In the following study, we evaluate how close ensemble averages from the partly filled matrix is to an emulated full matrix, and how these two methods for ensemble averaging compare to a hypothetical full simulation matrix.

The procedure adopted in collaboration with the ECMWF has been to select sub-matrices, or slices, in the matrix and as far as possible fill those. This decision at the beginning of the project was made through expert judgement. On the one hand, the existence of filled sub-matrices was a prerequisite for the development of the ANOVA-based hole-filling algorithm, but on the other hand, the direct ensemble average, taken over all existing simulations, gives a rather unequal weighting between the various GCMs and also the various RCMs in the matrix.

During the PRINCIPLES project, the GCMxRCM matrix of EURO-CORDEX regional climate projections has been extended considerably. A total of 66 simulations have brought the complete EURO-CORDEX to a total of 137 simulations (Table 1.1), with RCP8.5 accounting for 78 (of which one is still incomplete), RCP4.5 for 26 and RCP2.6 for 33 simulations.

In this study we aim at investigating the robustness of this matrix; in particular, we will use the ANOVA-based hole filling technique described in PRINCIPLES deliverable D1.4.1 and in Christensen and Kjellström 2020 and 2021.

Parallel ANOVA analyses of the entire RCPxGCMxRCM matrix are reported in Evin et al. (2021). Some differences in the method applied lead to somewhat different end results. Most importantly, the authors analyse all scenarios as one 3-dimensional matrix. This leads to decreased performance for the very populated RCP8.5 matrix but presumably to correspondingly better results for the other scenarios, which have not been analysed in the present report.

The existing simulations in the complete matrix in Table 1.1 at the time of this analysis number 77, 26, and 33 for the three scenarios considered. In this report we will only study the most populated matrix, the one following RCP8.5. We have furthermore chosen to use only one ensemble member for the three-member ensembles obtained from EC-EARTH and MPI-ESM-LR. We have skipped four of the

simulations driven by CNRM-CM5, where a particular boundary file error gave erroneous results (CNRM 2018). We have also skipped the single downscaling simulation of the GCM IPSL-IPSL-CM5A-LR for robustness. One planned simulation in the project (CNRM-CM5_RegCM4.6.1) was not complete at the time of writing. We are therefore in a situation where we can analyse a matrix of 8 GCMs and 11 RCMs (Table 1.2) populated with 58 existing simulations out of the 88 possible combinations (Table 1.3).

Table 1.1 Combination matrix between GCM and RCM choices for each of three RCP scenarios. Dark grey signifies non-PRINCIPLES simulations, dark green signifies PRINCIPLES simulations, where the number "1" indicates that the simulation was completed and available at the time of writing. Dark blue squares contain downscaled simulations from several GCM ensemble members, and are combinations of PRINCIPLES and non-PRINCIPLES simulations.

RCP8.5	RCA4	CCLM4-8-17	crCLIM	REMO 09,15	RACMO22E	HIRHAM5	WRF361H	WRF381P	ALADIN53	ALADIN63	RegCM4.6.1	HadREM3-GA7.05	ALARO-0	Total by GCM
MOHC-HadGEM2-ES	1	1	1	1	1	1	1	1		1	1	1		11
ICHEC-EC-EARTH	3	1	3	1	3	3	1	1			1	1		18
CNRM-CERFACS-CNRM-CM5	1	1	1	1	1	1		1	1	1		1	1	10
NCC-NorESM1-M	1		1	1	1	1		1		1	1	1		9
MPI-M-MPI-ESM-LR	3	1	3	3	1	1	1	1		1	1	1		17
IPSL-IPSL-CM5A-MR	1			1	1	1		1						5
IPSL-IPSL-CM5A-LR				1										1
CCCma-CanESM2		1		1										2
MIROC-MIROC5		1		1			1							3
Total by RCM	10	6	9	11	8	8	4	6	1	4	4	5	1	77
Remaining	0		0	0	0	0		0		0	1	0		1
RCP4.5	RCA4	CCLM4-8-17	crCLIM	REMO 09,15	RACMO22E	HIRHAM5	WRF361H	WRF381P	ALADIN53	ALADIN63	RegCM4.6.1	HadREM3-GA7.05	ALARO-0	Total now
MOHC-HadGEM2-ES	1	1		1	1	1								5
ICHEC-EC-EARTH	1	1		1	2	1								6
CNRM-CERFACS-CNRM-CM5	1	1			1				1	1			1	6
NCC-NorESM1-M	1			1		1								3
MPI-M-MPI-ESM-LR	1	1		2										4
IPSL-IPSL-CM5A-MR	1							1						2
Total by RCM	6	4	0	5	4	3		1	1	1	0	0	1	26
Remaining	0		0	0	0	0		0		0	0	0		0
RCP2.6	RCA4	CCLM4-8-17	crCLIM	REMO 09,15	RACMO22E	HIRHAM5	WRF361H	WRF381P	ALADIN53	ALADIN63	RegCM4.6.1	HadREM3-GA7.05	ALARO-0	Total now
MOHC-HadGEM2-ES	1			1	1	1					1	1		6
ICHEC-EC-EARTH	1	1		1	1	1						1		6
CNRM-CERFACS-CNRM-CM5				1	1				1	1			1	5
NCC-NorESM1-M	1			1	1						1			4
MPI-M-MPI-ESM-LR	1	1		2	1		1				1			7
IPSL-IPSL-CM5A-MR				1										1
IPSL-IPSL-CM5A-LR				1										1
NOAA-GFDL-ESM2G				1										1
MIROC-MIROC5		1		1										2
Total by RCM	4	3	0	10	5	2	1	0	1	1	3	2	1	33
Remaining	0		0	0	0	0		0		0	0	0		0
Total outside PRINCIPLES	13	13	0	18	10	5	5	1	3	0	0	0	3	71
Remaining all RCPs	0		0	0	0	0		0		0	1	0		1
PRINCIPLES total	7		9	8	7	8		6		6	8	7		66
Grand total	20	13	9	26	17	13	6	7	3	6	8	7	3	137

Table 1.2. The GCMs and RCMs participating in C3S_34b_Lot 2, which have been analyzed here.

GCMs	**Reference**
HadGEM2-ES	Collins et al., 2011
EC-EARTH	Hazeleger et al., 2012
CNRM-CM5	Voldoire et al., 2013
NorESM1-M	Bentsen et al., 2013
MPI-ESM-LR	Raddatz et al. (2007)
IPSL-CM5A-MR	Dufresne et al. (2013)
CanESM2	Chylek et al. (2011)
MIROC5	Watanabe et al. (2010)
RCMs	
RCA4	Samuelsson et al., 2011
CCLM4-8-17	Rockel et al., 2008
crCLIM	Leutwyler et al., 2017
REMO2015	Jacob et al., 2012
RACMO22E	van Meijgaard et al., 2008, 2012
HIRHAM5	Christensen et al., 2006
WRF361H	Skamarock and Klemp, 2008
WRF381P	Skamarock and Klemp, 2008
ALADIN63	Nabat et al., 2020
RegCM4.6.1	Giorgi et al., 2012
HadREM3-GA7.05	Walters et al., 2019

Table 1.3 Simulations analysed in the present report (dark green). A few simulations with technical problems have been excluded; also the RCMs with only one simulation have been excluded to keep the analysis robust. Finally, only the most frequently downscaled GCM ensemble member has been selected from the dark blue squares of Tab. 1.1.

RCP8.5	RCA4	CCLM4-8-17	crCLIM	REMO 09,15	RACMO22E	HIRHAM5	WRF361H	WRF381P	ALADIN63	RegCM4.6.1	HadREM3-GA7.05	Total by GCM
MOHC-HadGEM2-ES	1	1	1	1	1	1	1	1	1	1	1	11
ICHEC-EC-EARTH	1	1	1	1	1	1	1	1		1	1	10
CNRM-CERFACS-CNRM-CM5			1	1	1	1		1	1		1	7
NCC-NorESM1-M	1		1	1	1	1		1	1	1	1	9
MPI-M-MPI-ESM-LR	1	1	1	1	1	1	1	1	1	1	1	11
IPSL-IPSL-CM5A-MR	1			1	1	1		1				5
CCCma-CanESM2		1		1								2
MIROC-MIROC5		1		1			1					3
Total by RCM	5	5	5	8	6	6	4	6	4	4	5	58

Following Christensen and Kjellström (2020), an Analysis of Variance (ANOVA) has been performed on the RCP8.5 driven simulations. In this report we do not include interannual variability and therefore don't deal with the ANOVA-based significance calculations studied in Christensen and Kjellström (2020); rather, we concentrate on the practical usefulness of the method to potentially improve estimates of ensemble averages.

In this approach, we look at the influence from the choice of period (present or future, chosen as 1981-2010 and 2071-2100, respectively), of GCM and of RCM, where we analyse each field, each spatial point and each season separately. This is done by writing a simulation value Y_{ijk} from period *i*, GCM *j*, RCM *k* as

$$Y_{ijk} = M + S_i + G_j + R_k + SG_{ij} + SR_{ik} + GR_{jk} + SGR_{ijk} \quad (1)$$

i.e., as a sum of a mean (*M* over both periods and all GCM-RCM combinations), an average climate change contribution (*S*; really half the climate change, as it is defined as the deviation of one period, present-day or future, from the average of both periods), an average contribution from each individual GCM (G_j) relative to the average and a corresponding RCM contribution (R_k), (half the) GCM and RCM contributions to climate change (SG_{1j} and SR_{1k}), a cross term for an individual simulation's deviation from the before-mentioned averaged terms (*GR*), and a corresponding climate change cross term (*SGR).* Each term is defined to sum to zero over any index, leading to the expressions in Table 1.4.

The analysis has been performed for each grid point, each season, and for seasonal averages of temperature, precipitation, mean wind speed and incoming solar radiation.

Table 1.4 Formulae for the various ANOVA terms, under the requirement that all terms sum to zero over any single index. Dots indicate mean over indices.

Grand ensemble mean	M	$Y_{....}$
Scenario effect (climate change)	S_i	$Y_{i...} - Y_{....}$
GCM climate effect	G_j	$Y_{.j..} - Y_{....}$
RCM climate effect	R_k	$Y_{..k.} - Y_{....}$
GCM climate change effect	SG_{ij}	$Y_{ij..} - Y_{i...} - Y_{.j..} + Y_{....}$
RCM climate change effect	SR_{ik}	$Y_{i.k.} - Y_{i...} - Y_{..k.} + Y_{....}$
GCM-RCM cross term for mean	GR_{jk}	$Y_{.jk.} - Y_{.j..} - Y_{..k.} + Y_{....}$
GCM-RCM cross term for change	SGR_{ijk}	$Y_{ijk.} - Y_{ij..} - Y_{i.k.} - Y_{.jk.} + Y_{i...} + Y_{.j..} + Y_{..k.} - Y_{....}$

In the current situation with a matrix not completely filled, i.e., with holes, we will follow Christensen and Kjellström (2021) setting the individual cross terms *GR* and *SGR* to zero and use the equation system of Eq. 1 to solve for the values in the holes. Setting those terms to zero indicates that we cannot have any knowledge of cross terms characterizing individual simulations, which have actually not been performed; note that all terms sum to zero over each explicit index. The emulated values in the matrix

will not contribute to the part of the ensemble variation normally present in these terms, specifically the internal variability, which will therefore be reduced compared to a matrix completely populated with actual simulations. We will end up with emulated values for the holes, which are sums of GCM and RCM contributions for the combination in question.

Taking ensemble averages of fields across the completed matrix, with emulated values in the holes, will result in values where each participating GCM as well as each participating RCM will have an equal weight, independent of the actual number of simulations performed with this model. We note that, the method does not give any information on GCMs and RCMs that have not been included in the analysis.

1.2 Results for seasonal averages

In the present situations we have 88-58=30 linear equations with 30 unknowns, the field values in the holes. The linear equation matrix only depends on the configuration of holes and can therefore be inverted once and then applied to each point and season. The equations are readily solvable due to the inter-connectedness of the GCMxRCM matrix: it cannot be split into non-overlapping sub-matrices; there are several existing simulations for all participating models, GCMs as well as RCMs. Below, we present results for winter (DJF) and summer (JJA) for seasonal-average surface air temperature, total precipitation, and average 10m wind speed.

1.2.1 Temperature

In Fig. 1.1 we show winter and summer temperature change between the periods investigated, 12/1980-11/2010 and 12/2070-11/2100 (chosen to each contain 30 whole seasons of each kind). The ensemble mean is taken as: i) a direct average over all 58 RCP8.5 simulations in Table 1.3 or ii) as an average over the complete 88 combinations including the 30 emulated values. We see the well-known patterns: strongest winter warming in the north-east, and strongest summer warming in the south of Europe.

The robustness of the results is illustrated through the comparison between the direct mean and the mean of the complete matrix, filled out with emulated values in all holes. Fig. 1.2 shows the difference between the emulated and the direct ensemble means in Fig. 1.1. These differences are at most 10% of the climate change, and there is only very small visible differences between the maps Fig. 1.1 and corresponding maps with the alternative averaging method (not shown).

Still, we want to understand where the slightly increased warming in the emulated mean comes from. In Figs 1.3 and 1.4 we show temperature change for summer and winter, respectively, averaged over the entire domain for each individual simulation, including emulated values. The ensemble mean value has been subtracted. It is clear that the GCM is the dominant parameter for the degree of warming (see the consistency in patterns for the GCM rows in Fig. 1.3).

A comparison of the two panels of Fig. 1.3 indicates that two GCMs with several holes, IPSL-CM5A-MR and CanESM2, are quite warm and at the same time have several holes; the coldest GCMs, NorESM1-M and MPI-ESM-LR are well populated with actual simulations and therefore do not gain weighting from as many added emulated values. The more “democratic” weighting of the full, emulated matrix gives more weight to these simulations. Exactly the same arguments apply to the summer situation (Fig. 1.2) where we see roughly the same distribution of warming between GCMs as for winter, with the two above-mentioned GCMs being warmer than the GCM ensemble average (Fig 1.4).

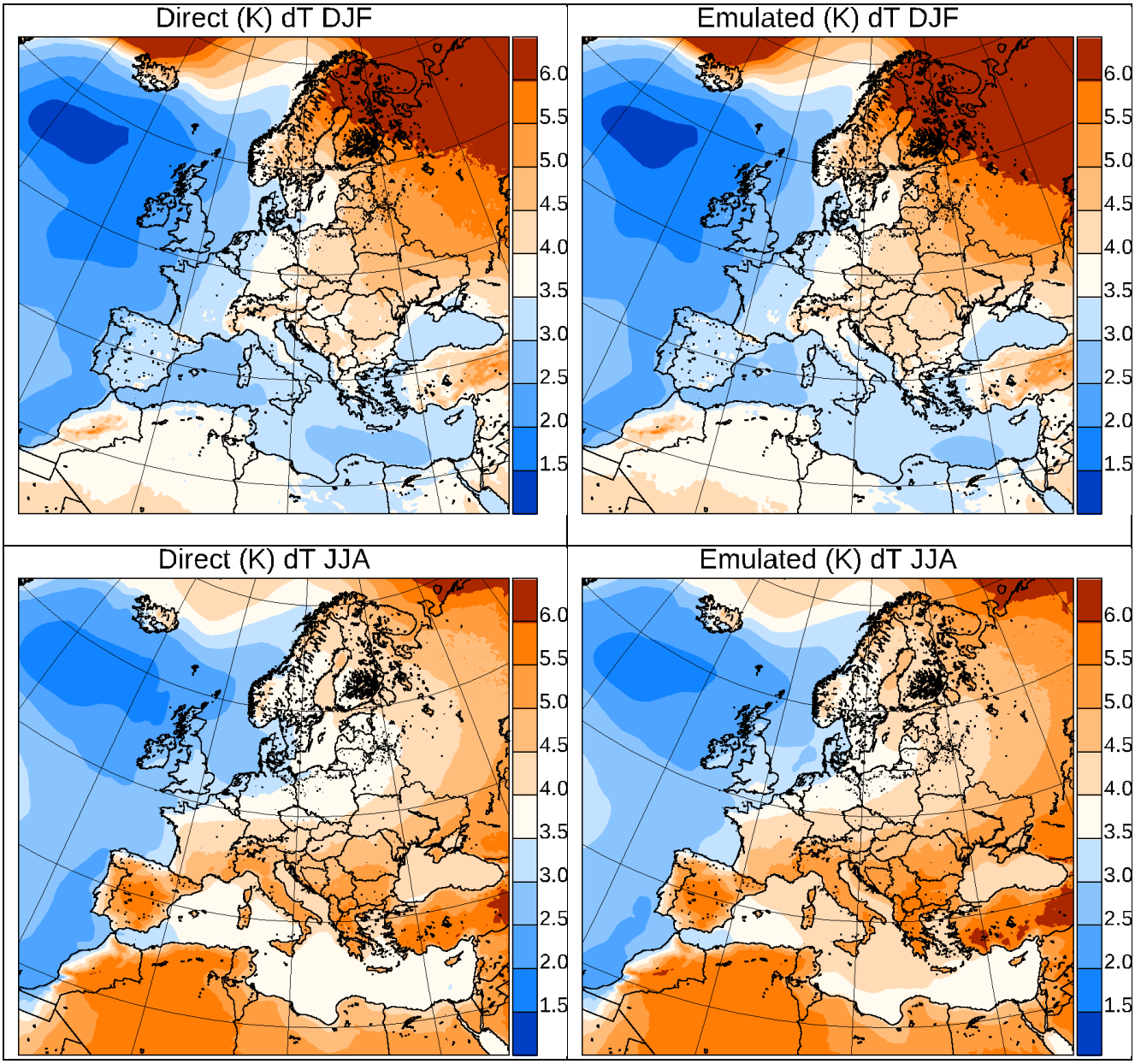

Figure 1.1 Temperature change (K) calculated directly (left column) from the existing 58-member ensemble or from the full 88-member emulated matrix (right column). Top panels: Winter (DJF); bottom panels: Summer (JJA).

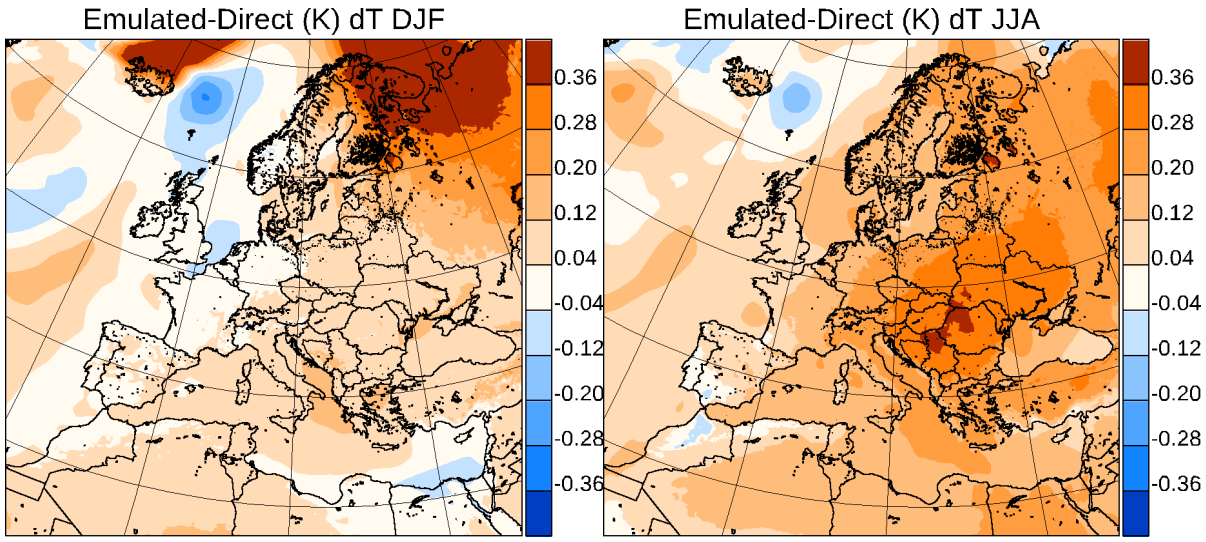

Figure 1.2 Temperature change difference (K) between ensemble means calculated directly from the existing ensemble and from the full emulated ensemble. Left panel: Winter (DJF); right panel: Summer (JJA). Note the much smaller level intervals compared to Fig. 1.1.

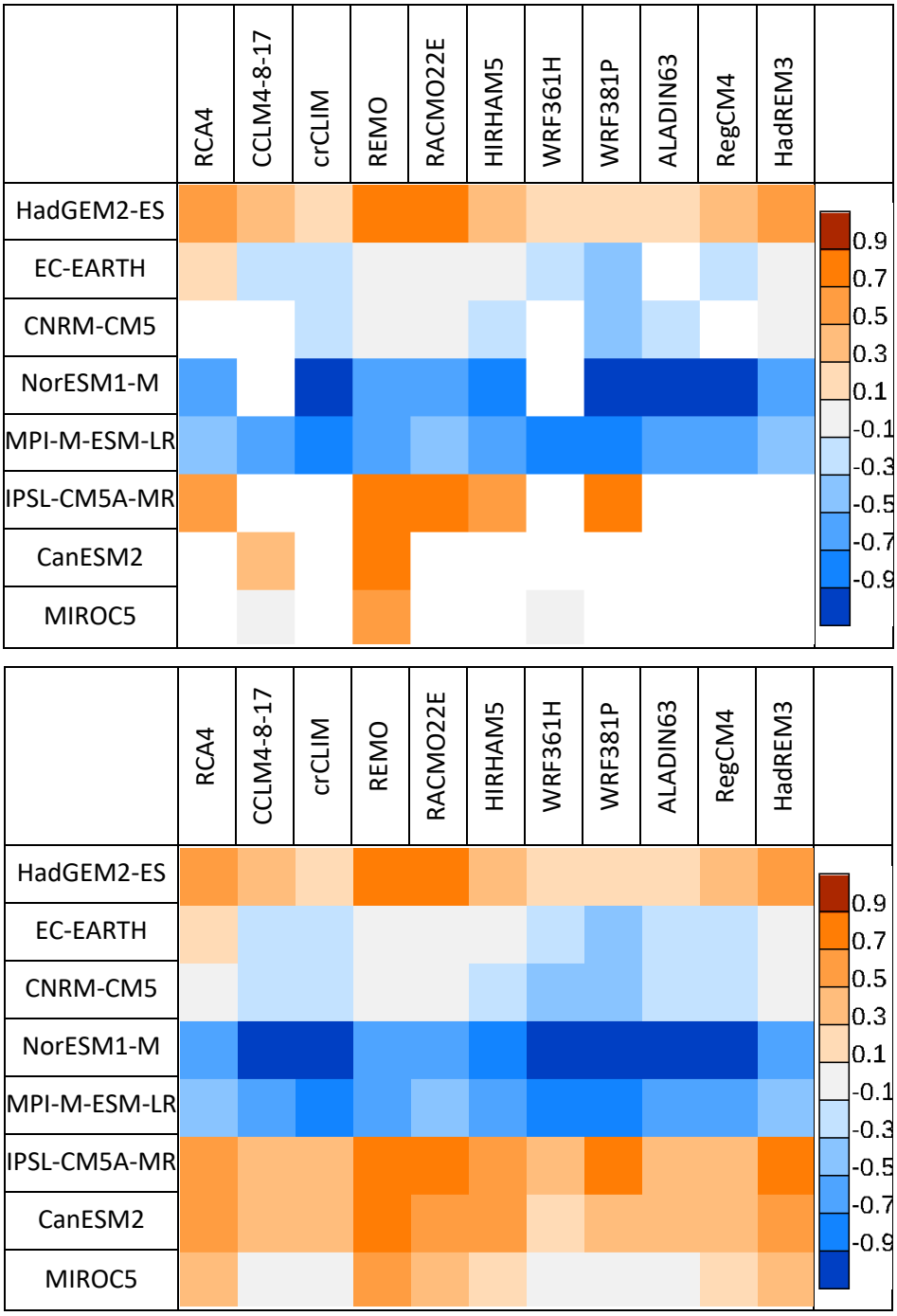

Figure 1.3 Winter domain-averaged temperature change relative to the ensemble average (K). Top panel: Existing simulations only. Bottom panel: With emulated values for holes. Note that white colour in the top panel indicates a missing simulation, as opposed to the grey colour for numerically small temperature changes.

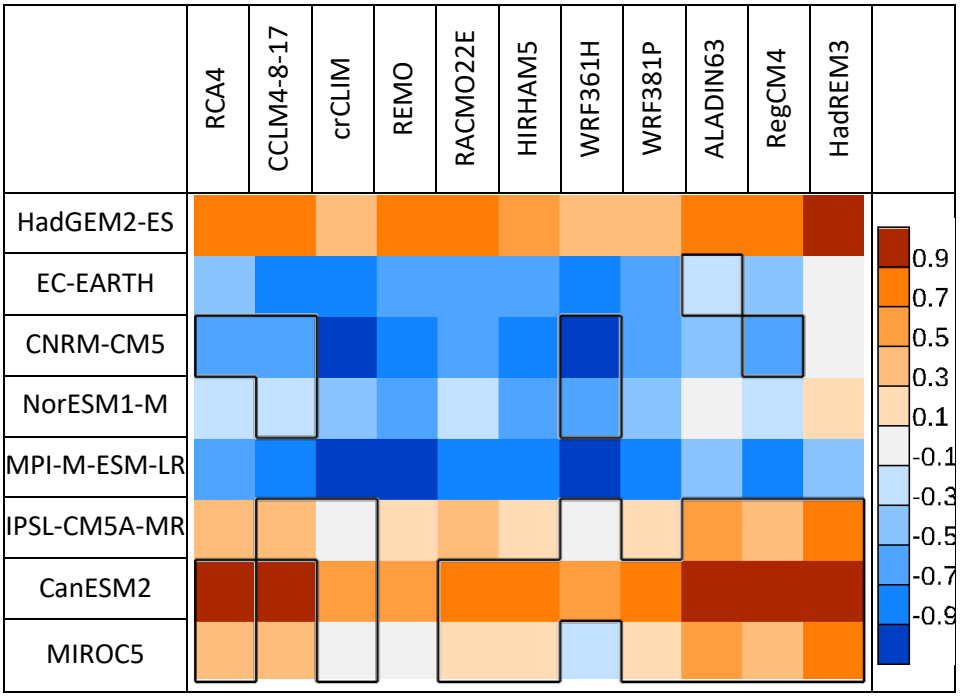

Figure 1.4 Summer domain-averaged temperature change relative to the ensemble average (K). With holes filled. Positions with emulated values are framed (cf. Fig. 1.3).

1.2.2 Precipitation

In the case of precipitation, we study the relative change from control to future periods, measured in per cent. In Fig. 1.5 we show the relative precipitation change for both methods of obtaining an ensemble average. In Fig. 1.6 we show the differences between the two averaging methods for this quantity, i.e., measuring this difference in percentage points. The large regions with large differences in relative change between the two methods in Fig. 1.6 are regions with very little precipitation, like northern Africa and the Iberian Peninsula in summer, which means that the relative climate change does not correspond to a large difference in absolute precipitation amount. Also, the method differences are hardly noticeable in Fig. 1.5, as they are much smaller than the geographical variation.

Fig. 1.7 shows the relative change in area-averaged precipitation for each simulation compared to the ensemble average.

As for temperature, GCMs seem to play a larger role for the climate change signal than RCMs, with WRF361H being a notable exception (see the RCM column of WRF361H in Fig. 1.7). For winter, the three GCMs with the fewest existing simulations (IPSL-CM5A-MR, CanESM2, and MIROC5) are all outliers, but in different directions (IPSL-CM5A-MR and CanESM2 are wetter and MIROC5 is drier). Also, the WRF361H RCM, which has several holes, shows an anomalously negative signal for most drivers compared to the ensemble mean change. Looking at the GCMs with few actual simulations, i.e., the GCMs whose signal will have the largest contribution to the difference between the two methods, there are opposing contributions: the GCMs IPSL-CM5A and CanESM2 show relatively large

precipitation increase, whereas MIROC5 shows a decrease in precipitation between the two time slices studied (not shown).

In summer, the relative importance of the RCM is visibly larger than in winter. This is expected, as summer precipitation is determined by local processes to a higher extent than the predominantly cyclone-determined winter precipitation. There is a much higher inter-model variability. There are still some models with systematic deviations from the average. On the RCM side, WRF381P is particularly wet, whereas CCLM4-8-17 is dry. For GCMs, MIROC is systematically wet, while NorESM is rather dry.

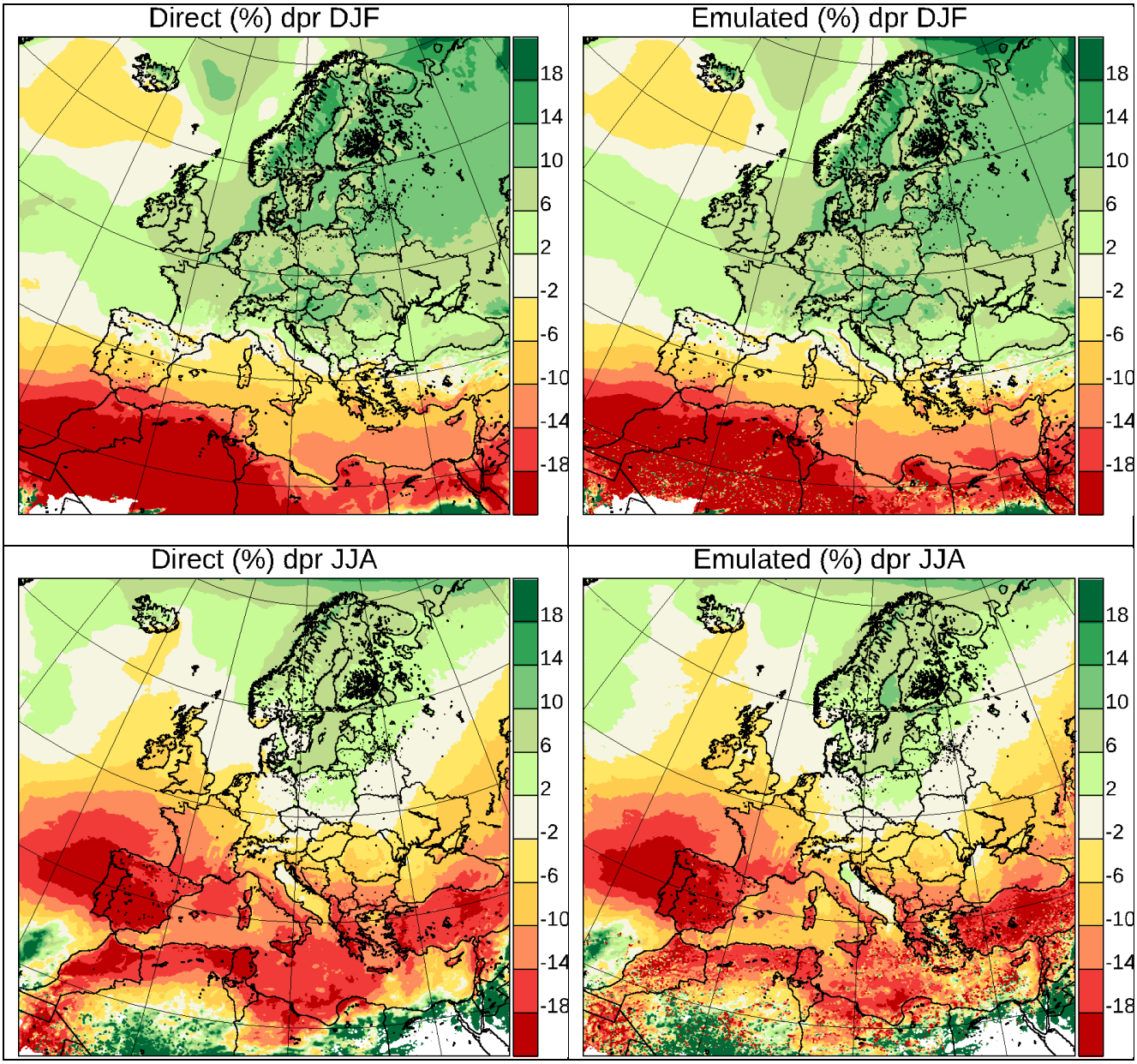

Figure 1.5 Precipitation change (%) calculated directly (left column) from the existing ensemble or from the full emulated matrix (right column). Top panels: Winter (DJF); bottom panels: Summer (JJA).

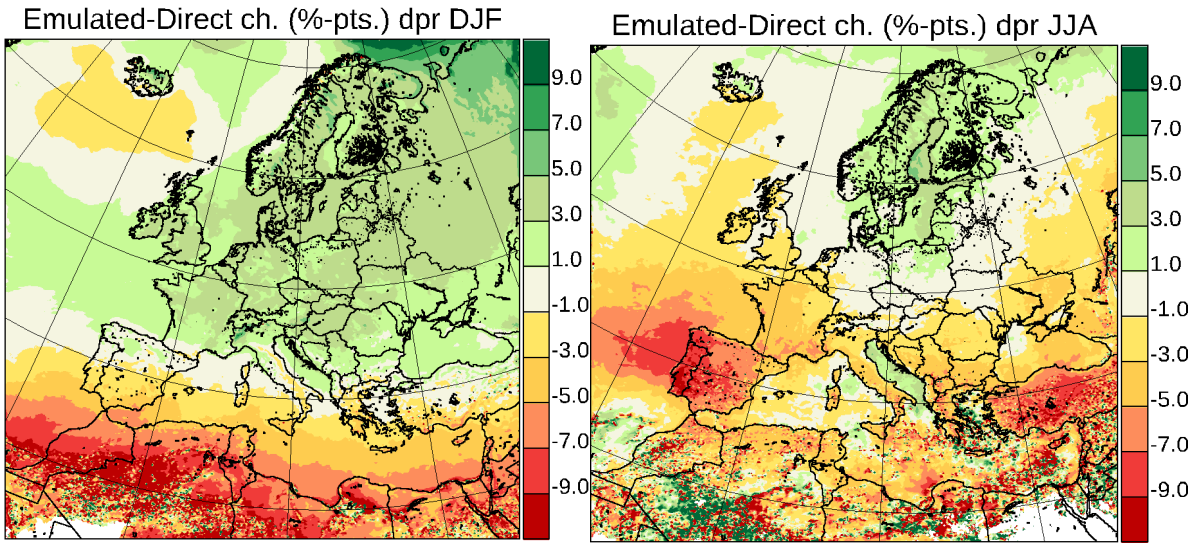

Figure 1.6 Relative precipitation change (%-points) difference between ensemble means calculated directly from the existing ensemble and from the full emulated ensemble. Left panel: Winter (DJF); right panel: Summer (JJA).

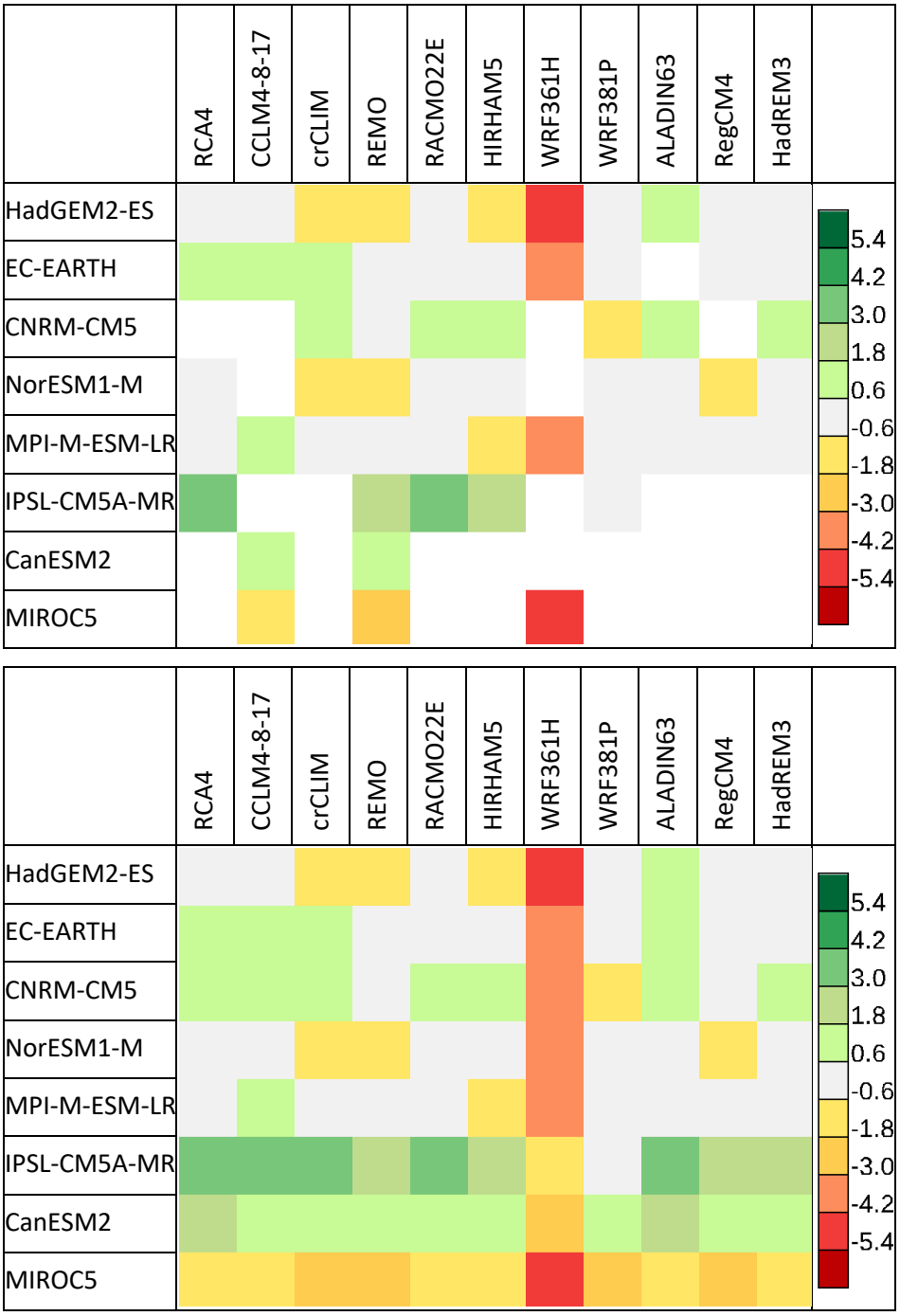

Figure 1.7 Winter domain-averaged precipitation relative change minus the ensemble average (%-points). With holes filled. Top panel: Existing simulations only. Bottom panel: With emulated values for holes. Note that white colour in the top panel indicates a missing simulation, as opposed to the grey colour for numerically small precipitation changes.

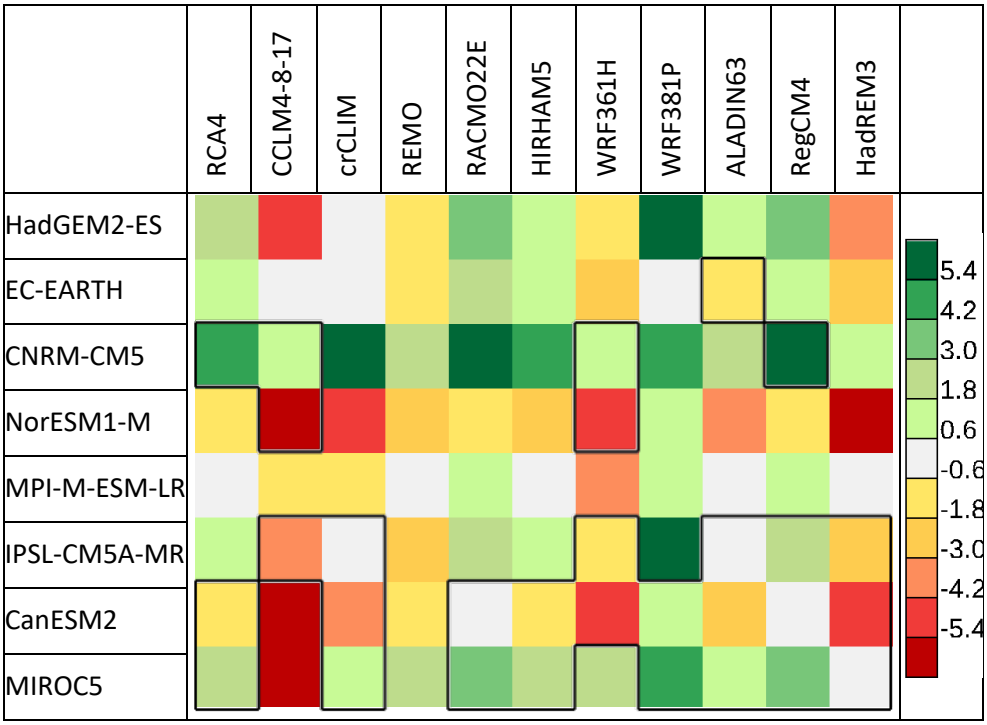

Figure 1.8 Summer precipitation relative change minus the ensemble average (%-points). Full emulated ensemble. Positions with emulated values are framed (cf. Fig. 1.3).

1.2.3 Wind speed

The daily average wind speed at 10 m has been analysed in the same way as precipitation (considering changes in percentage). In Figs 1.9-1.12 we show the results in similar way as Figs 1.5-1.8. There are generally more negative changes for the emulated ensemble, but these differences are hardly visible.

In Figs 1.11-1.12 we see mostly horizontal stripes for winter and both horizontal and vertical striping for summer, indicating that the GCM-generated large-scale weather is more important in winter vs. local effects being more important in summer.

Even though Figs 1.11-1.12 only show results for the entire integration domain, it seems plausible that the MIROC5 GCM and the WRF381P RCM, which both have several holes and also have anomalously negative results, would be the reason for the negative winter differences in Fig. 1.10, left panel.

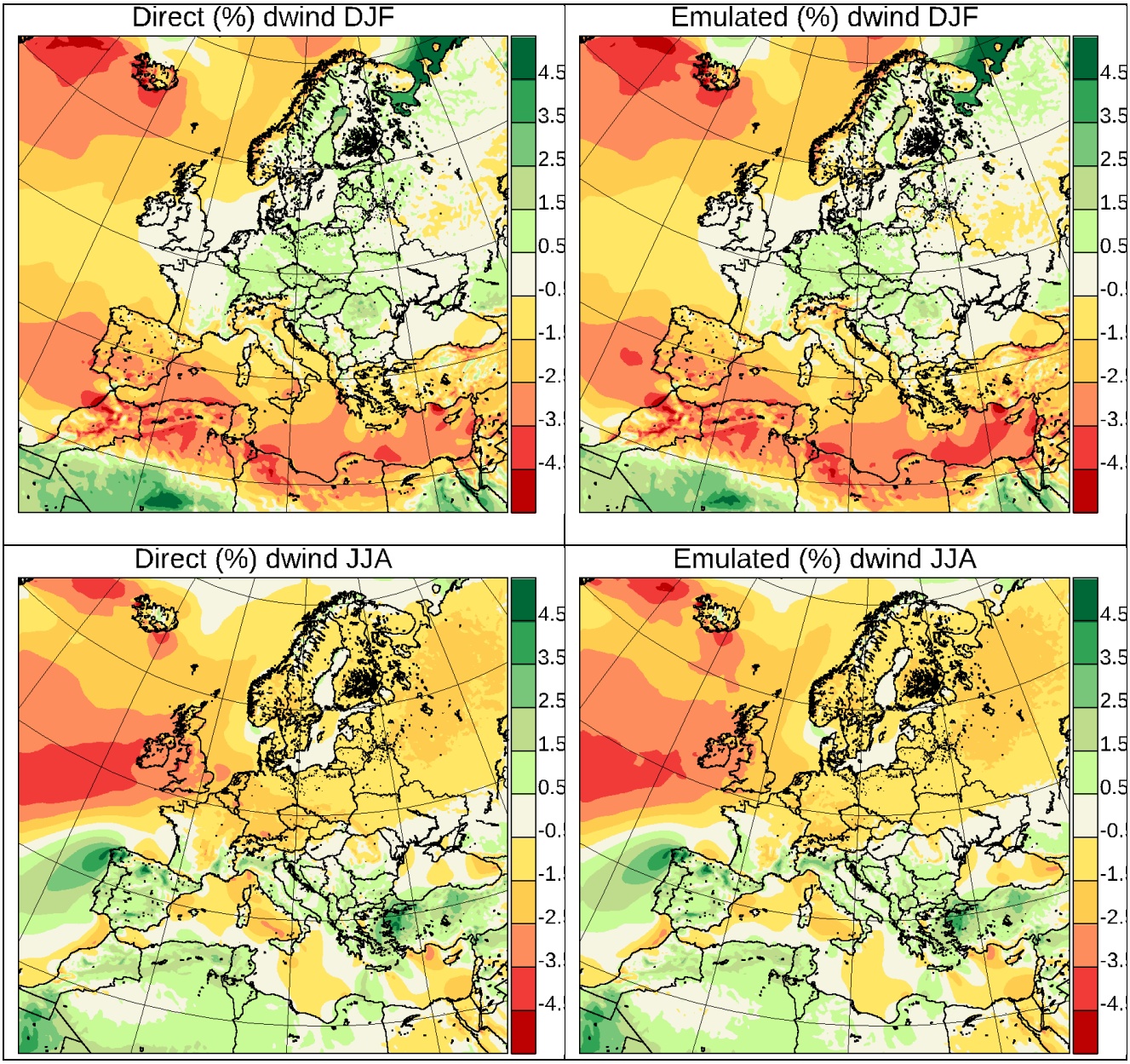

Figure 1.9 Wind speed change (%) calculated directly (left column) from the existing ensemble or from the full emulated matrix (right column). Top panels: Winter (DJF); bottom panels: Summer (JJA).

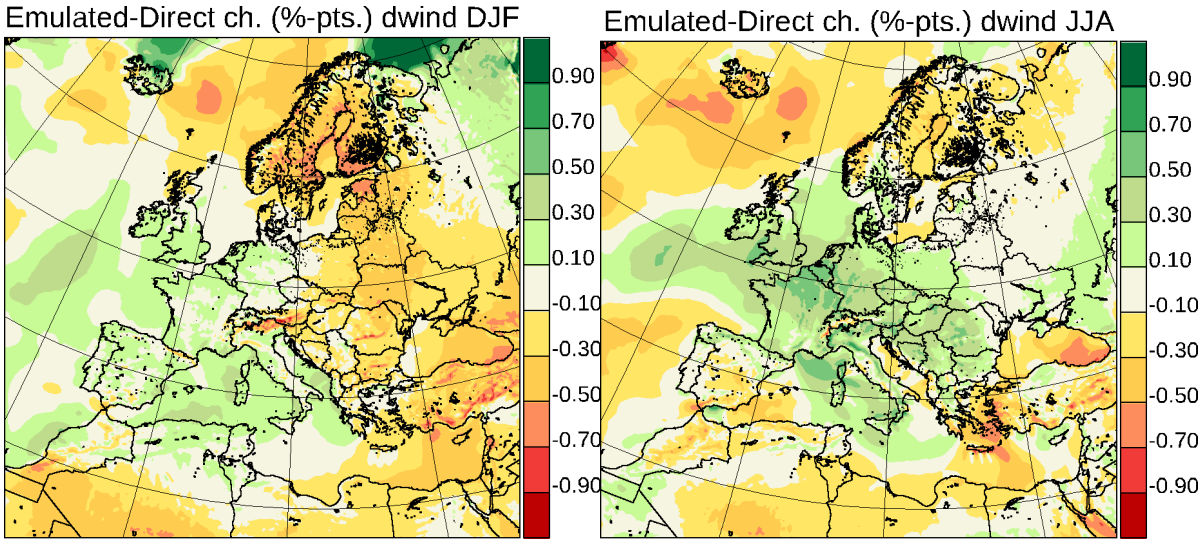

Figure 1.10 Relative 10m wind speed change (%-points) difference between ensemble means calculated directly from the existing ensemble and from the full emulated ensemble. Left panel: Winter (DJF); right panel: Summer (JJA).

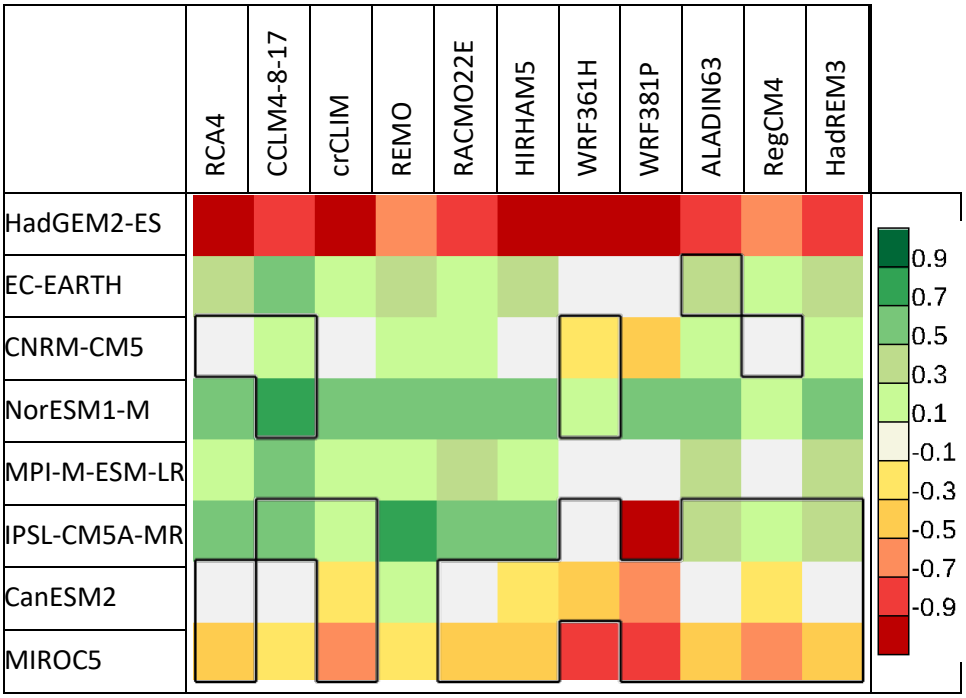

Figure 1.11 Winter domain-averaged wind relative change minus the ensemble average (%-points). With holes filled. Positions with emulated values are framed (cf. Fig. 1.3).

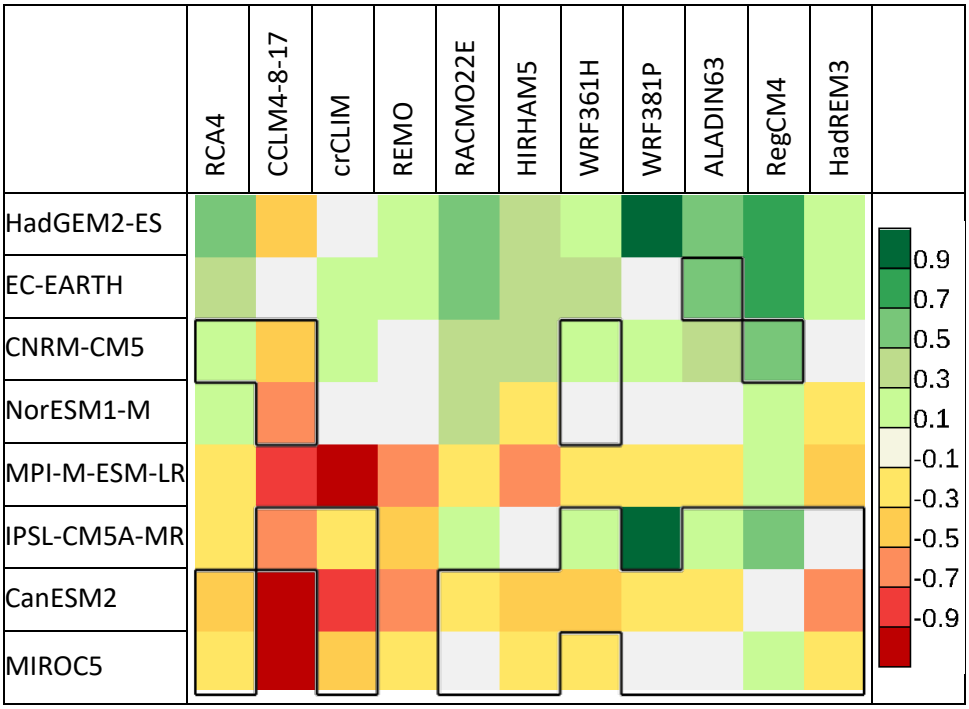

Figure 1.12 Summer domain-averaged wind relative change minus the ensemble average (%-points). With holes filled. Positions with emulated values are framed (cf. Fig. 1.3).

1.2.4 Ensemble means

A central question is to determine how large the effect of the missing simulations is on the climate change signal. We cannot answer this question directly, as these simulations are missing, but we can apply the equations that were set up in Christensen and Kjellström (2021) to obtain an estimate. These equations describe the expected root-mean-square deviation between a true full-ensemble average and averages of synthetically filled matrices, including emulated numbers, as well as direct averages of existing simulations in the incomplete matrix. The estimates from this study were obtained by successively degrading a 5x4 fully populated sub-matrix of the EURO-CORDEX RCP8.5 matrix, analysing all possible configurations of matrices with specific numbers of holes; the equation will not necessarily apply exactly to a specific individual matrix; in the current study we apply it to the specific existing EURO-CORDEX RCP8.5 matrix. Furthermore, the ANOVA terms used in the estimates are the perfect full-matrix terms, whereas we, in the present situation, only have our best estimate from the emulation process. However, in spite of these caveats, we do get estimates of this deviation for each point and season. We show these RMS deviations for climate change as calculated for the three fields (temperature, precipitation, and 10 m wind speed) and two seasons (winter and summer) in Figs 1.13-1.15.

Due to the formulation of the ANOVA method, the climate change signal is measured in absolute units, and not in percent as above.

The estimate is expressed for climate change in Eq. 2 (Christensen and Kjellström, 2021; note the factor of 2 since we calculate climate change, while Christensen and Kjellström (2021) calculate the scenario

minus the period mean), where $N_G = 8$ is the number of GCMs, $N_R = 11$ is the corresponding number of RCMs, $N = N_G * N_R$ = 88 and *m*=30 is the number of holes in the matrix. $\langle SGR^2 \rangle$ in Christensen and Kjellström (2021) is the average over many different configuration matrices with *m* holes of the squared *SGR* term, here replaced by the *SGR* term resulting from the solution of the hole-filling Eq. 1. In Eq. 3 we show the corresponding estimate of the simple, direct average's RMS deviation (denoted by D). For details, see Christensen and Kjellström (2021).

$$D_{emulated}(m) = \frac{2\sqrt{\langle SGR^2 \rangle}}{(N_G - 1)(N_R - 1)} \frac{\sqrt{m}\,(N-1)}{N-m} \tag{2}$$

$$D_{direct}(m) = \frac{\sqrt{\langle SG^2 + SR^2 + SGR^2 \rangle}}{(N-1)} \sqrt{\frac{m\,(N-1)}{N-m}} \tag{3}$$

It should be noted that the corresponding equation for the direct mean indicates that emulation is quite advantageous in the current situation, since the ratio between the two methods is proportional to $\sqrt{\frac{\langle SGR^2 \rangle}{\langle SG^2+SR^2+SGR^2 \rangle}}$ which is generally quite small for "well behaved" average fields without dominating internal variability like the fields studied here; for extremes and other noisy fields, the ratio approaches unity, meaning that the emulation is actually worse than a direct average, due to the prefactor when dividing Eq. 2 with Eq. 3. This is equivalent to a statement that the linear splitting in the ANOVA procedure is working very well for the matrix and fields under investigation, describing a large fraction of the total variability. The estimated RMS deviation from the full matrix for the direct average is at least twice the deviation of the emulated average for temperature; the deviations are closer to each other but still better for the emulated average for precipitation and wind; hence, the method does add value to determination of ensemble averages for these fields. These relations between the two averaging methods are directly related to the ANOVA ratio mentioned above.

Without putting too much emphasis on the details of Figs 1.13-1.15, we do conclude that a full matrix would probably deviate less than 0.1 K for seasonal temperature change, less than 0.02 mm/day for seasonal precipitation change though up to 0.04 mm/day for coasts and mountain ranges, and below 0.01 m/s for seasonal mean wind speed change. In sea-ice covered regions like the Barents Sea, both winter temperature and winter wind speed deviations are relatively large, as observed in Christensen and Kjellström (2020) with a smaller ensemble. Sea ice represents a climate phenomenon where both the GCM calculating sea ice cover and the RCM formulating the boundary layer description play roles, which are not easily split into linear contribution from each type of models.

The comparison of absolute and not of relative change has important effects for wind. Two of the RCMs (RegCM3 and WRF381P) have large positive anomalies in wind speed, more than 15% in area average and much larger for mountainous areas, whereas two other RCMs (CCLM4-8-17 and crCLIM) have rather low wind speeds, though not quite as strong a deviation from the ensemble mean. This means that the absolute change in wind speed is very much determined by the RCM. A consequence

of this is that the emulated mean, which gives equal weight to each RCM, performs more than five times better than the direct ensemble mean.

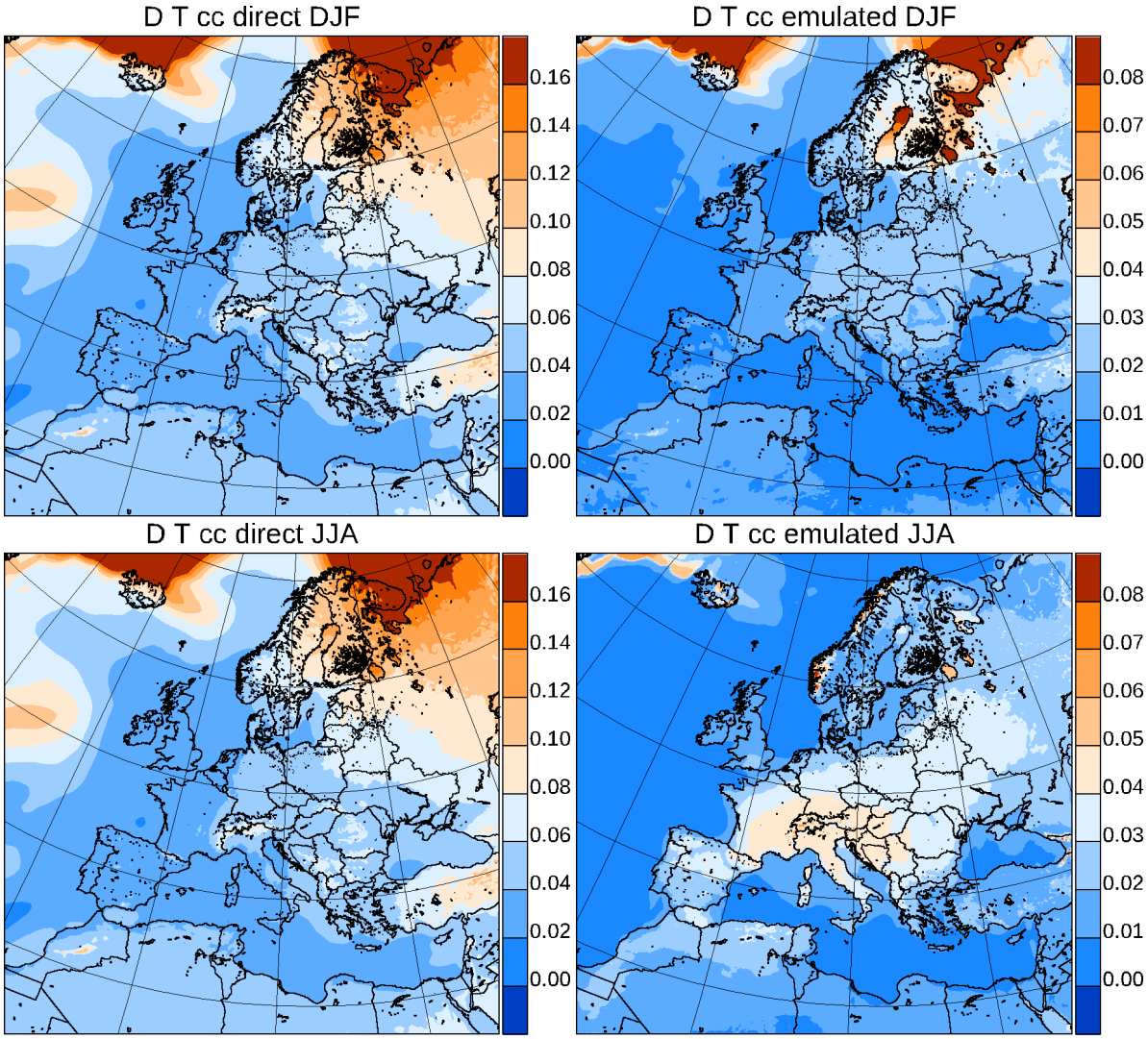

Figure 1.13 Estimated RMS deviation of temperature (K) direct (left column) and emulated (right column) ensemble mean from hypothetical full ensemble mean. Top row: Winter; bottom row: Summer. Note the different colour code definitions!

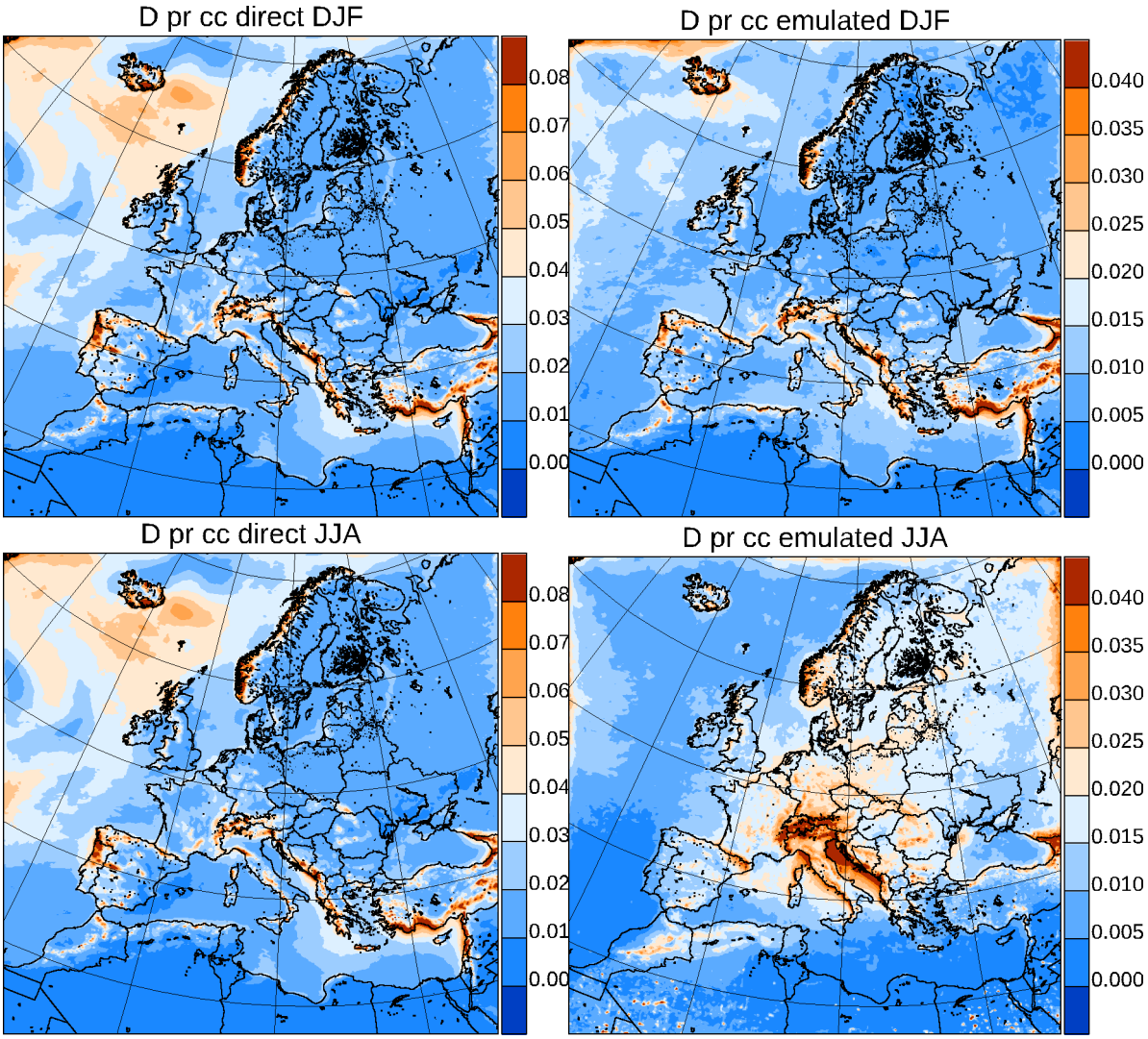

Figure 1.14 Estimated RMS deviation of precipitation (mm/day) direct (left column) and emulated (right column) ensemble mean from hypothetical full ensemble mean. Top row: Winter; bottom row: Summer. Note the different level definitions in the two columns!

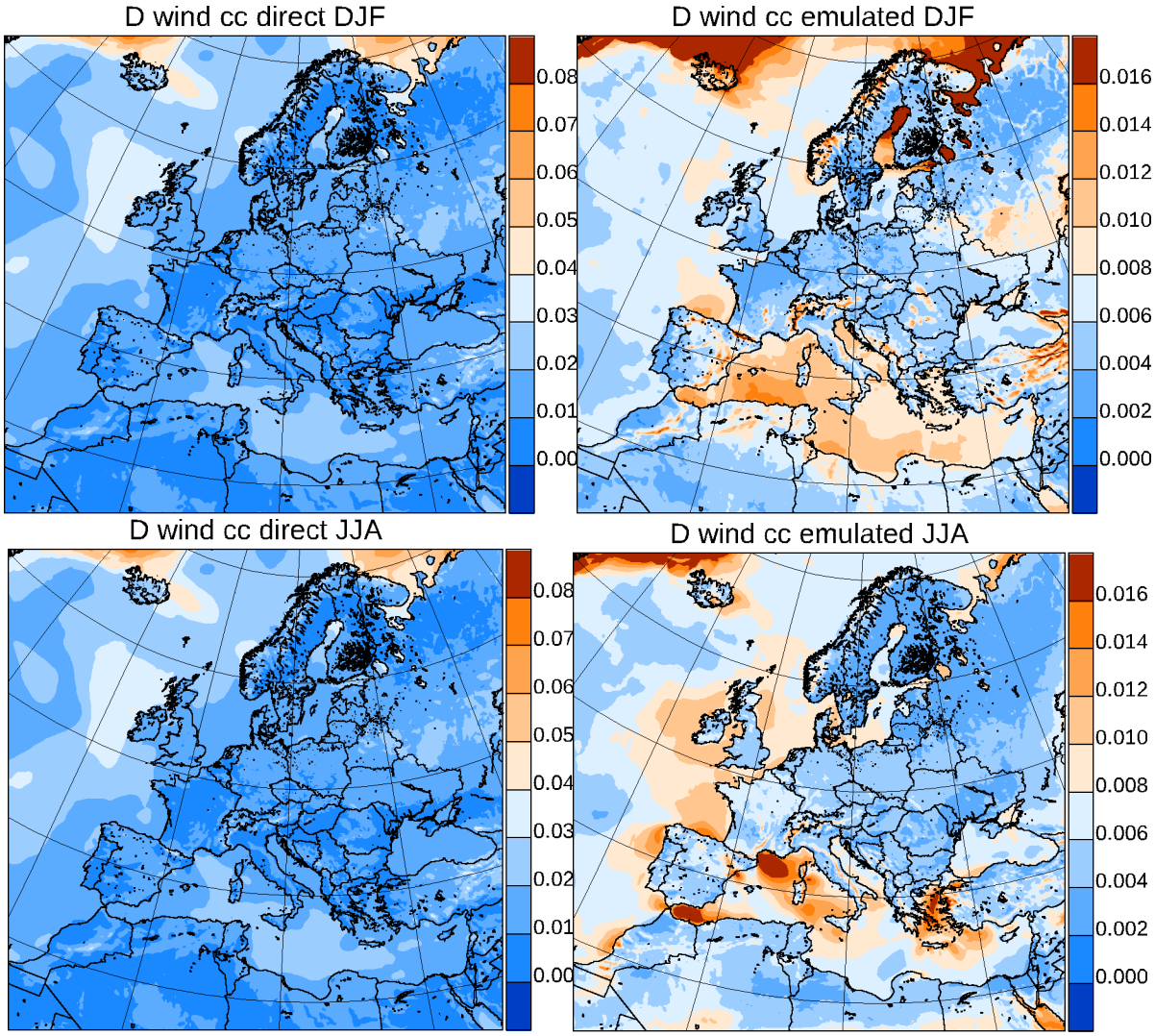

Figure 1.15 Estimated RMS deviation of wind speed (m/s) direct (left column) and emulated (right column) ensemble mean from hypothetical full ensemble mean. Top row: Winter; bottom row: Summer. Note the different level definitions in the two columns!

1.3 Conclusion and Perspective

The currently analysed GCMxRCM matrix for the RCP8.5 scenario is 66% full, with 58 out of 88 possible combinations done — 39 of which have been performed in this project. As the ANOVA-based matrix filling requires a minimum degree of filling in the matrix, which was not reached before PRINCIPLES for any sub-ensemble of comparable magnitude, such an assessment would not have been possible before the many simulations added in the PRINCIPLES project.

The investigation indicates that the ensemble averages, which can be obtained from the existing simulations, would be extremely close to the values of a filled matrix for seasonal-average 2m temperature, precipitation and 10m wind speed. With fewer simulations, down to the minimum ANOVA requirement of $N_G + N_R - 1 = 18$ simulations (see Christensen and Kjellström (2021)), the

deviation of an emulated matrix from a filled matrix would be considerably larger and less trustworthy. In the near future, artificial degradation of the full RCP8.5 matrix will be performed in order to study if the formulae obtained from degradation of a smaller but complete sub-matrix in Christensen and Kjellström (2021) are applicable here.

The ANOVA-based technique gives large relative improvements over direct averaging for all fields considered but these improvements are still small compared to the geographical variation of climate change and can be replaced by direct ensemble averages without large differences in results, due to the high degree of filling already present in the current matrix. We also note that, even if improvements are large in relative terms they are not necessarily large in absolute numbers as there is already quite good agreement already for the direct averaging, at least for this relatively densely filled matrix.

Ensemble averages are expected to be within 0.05 degrees of a hypothetical full-matrix seasonal-mean temperature for each point, except for slightly larger expected deviations in winter in the Barents Sea. For precipitation, the corresponding order of magnitude is 0.05 mm/day, mostly below 0.02 mm/day; for wind speed mostly below 0.01 m/s over land but with higher values over the Barents Sea in winter. The reason for the break-down of the method over sea ice filled regions is probably related to the direct interaction between GCM and RCM detailed description of physical mechanisms: the coupled GCM determines the sea ice cover, and the RCM calculates temperatures and other local fields based on this; we therefore see larger GCM-RCM cross terms for mean (*GR)* and change (*SGR)* in these areas than we generally do for the rest of the European domain.

The more sparsely populated RCP4.5 and RCP2.6 matrices would probably have larger expected deviations. This will be studied in the future.

This study has limitations. It is not expected that the ANOVA-based filling technique will work for variables with very large internal variability, as it is the case for extremes of precipitation and wind, since noise will make *GR* and *SGR* the dominant terms with most of the variability (Christensen and Kjellström, 2021). It is, however, important to study how well ensemble-averaged return values would compare to a more completely filled matrix.

2. Added value of PRINCIPLES simulations on European climate change signals in temperature and precipitation

2.1 Introduction

PRINCIPLES has contributed to the EURO-CORDEX ensemble extensively by providing a total of 66 Regional Climate Model (RCM) simulations under various Representative Concentration Pathways (RCP2.6, RCP4.5 and RCP8.5). The EUR-11 subset – at a horizontal resolution of 12 km – currently represents the largest available RCM ensemble, with a systematically and densely filled RCP-GCM-RCM matrix for a total of 136 simulations (see Table 1.1). In the past, the assessment of climate change was largely based on RCM ensembles of opportunity, which made it hard to assess the uncertainty of the respective climate projections. The PRINCIPLES simulation matrix is based on a common set of 8 pre-selected Global Climate Models (GCMs). As it was not possible to fill the 3-dimensional RCP-GCM-RCM matrix entirely due to the high computational cost, the strategy followed by PRINCIPLES was to select and fill sub-matrices to allow an assessment of how the choice of RCM and GCM models contributes to the spread in the resulting ensemble (Christensen and Kjellström 2020, Vautard et al. 2020). Focus has been put on the RCP8.5 scenario for which 78 simulations are available in total (including simulations run outside of PRINCIPLES). The large PRINCIPLES RCM matrix now offers an exciting opportunity to assess European climate change projections, to evaluate the spread of the results, and to estimate the uncertainty and reliability of the projections.

In a previous study, Rajczak and Schär (2017) considered a large dataset of 100 European climate change simulations from several ensembles of opportunity (ENSEMBLES, EURO-CORDEX EUR-44 and a small available EUR-11) to investigate changes in precipitation mean, frequency, intensity and extremes under various climate scenarios. The authors found an overall increase in precipitation extremes in most parts of Europe throughout the year, an intensification of extremes in northern Europe in winter, and a decrease in mean precipitation but an increase in intense precipitation in southern Europe in summer, although the ensemble spread is large in summer. These climate change signals, based on somewhat old simulations, are similar to the recent study published through PRINCIPLES (Coppola et al. 2021), which increases our confidence in projections over Europe using the current generation of RCMs at 12 km resolution.

The current study takes advantage of the latest EUR-11 simulation ensemble, and provides a comparison against the smaller EUR-11 ensemble, which was already available before the start of PRINCIPLES. Through this study, we aim to quantify the additional information gained by filling the GCM-RCM matrix under the RCP8.5 scenario. Here, we present projected changes in mean temperature and mean and extreme daily precipitation and focus on a possible shift in the ensemble median and spread before and after PRINCIPLES. We do not address the biases of the simulations in the historical period, which was already assessed by Vautard et al. (2020). However, it is worth noting that previous studies found that GCM-RCM model chains generally have smaller biases than the raw

GCM simulations (Sørland et al. 2018 based on EURO-CORDEX simulations before PRINCIPLES, and Christensen and Kjellström 2020 based on PRINCIPLES simulations). The following results are preliminary and not published yet.

2.2 Methods

The study considers daily mean precipitation (pr) and seasonal mean temperature at 2m (tas) in EUR-11 regional climate simulations forced with the RCP8.5 scenario available at ESGF. These include EUR-11 simulations run before PRINCIPLES (24 simulations), as well as EUR-11 PRINCIPLES simulations (46 simulations), bringing a total of 70 simulations (Table 1.1). In total, there are 78 EUR-11 simulations, but we have not included in our analyses the PRINCIPLES simulations not published yet, or only recently published, on ESGF (the 3 green crosses in Table 2.1). Regarding the CNRM-CM5-forced RCM simulations, we have only included the simulations forced by CNRM-CM5 pressure level fields (5 RCP8.5 simulations, highlighted in grey in Table 2.1, are therefore excluded; see CNRM (2018) for more details).

For these analyses, the last 30 years of the simulations have been considered: 1981-2010 for the historical forcing, and 2070-2099 for the RCP8.5 forcing. The analyses have been performed over the PRUDENCE regions (Fig. 2.1; Christensen and Christensen 2007), and averaged over land points only. In terms of temperature, we focus on changes in mean temperature for now. In terms of precipitation, we consider changes in mean precipitation and changes in precipitation extremes, computed as the 99th percentile of all-day precipitation, following Rajczak and Schär (2017).

Table 2.1: All available EUR-11 simulations for the RCP8.5 scenario. Black crosses show simulations run before the start of PRINCIPLES. Grey crosses are CNRM-CM5-forced simulations not considered in this study (see details in the text). Red crosses show simulations run within PRINCIPLES. The green cross shows the PRINCIPLES simulation that is not available at ESGF yet and therefore not included in this study.

		RCM														
		CLMcom-CCLM4-8-17	KNMI-RACMO22E	SMHI-RCA4	DMI-HIRHAM5	IPSL-INERIS-WRF381F	UHOH-WRF361H	IPSL-INERIS-WRF381P	MPI-CSC-REMO2009	GERICS-REMO2015	CNRM-Aladin53	CNRM-Aladin63	ICTP-RegCM4-6	CLMcom-ETH-COSMO-crCLIM-v1-1	RMIB-Ugent-ALARO-0	MOHC-HadREM3-GA7
GCM	CNRM-CERFACS-CNRM-CM5	x	x	x	x	x		x		x	x	x	x	x	x	x
	MOHC-HadGEM2-ES	x	x	x	x		x	x		x		x	x	x		x
	ICHEC-EC-EARTH r12	x	x	x	x			x		x			x	x		x
	ICHEC-EC-EARTH r1		x	x	x		x							x		
	ICHEC-EC-EARTH r3		x	x	x									x		
	CCCma-CanESM2	x								x						
	MIROC-MIROC5	x					x			x						
	MPI-M-MPI-ESM-LR r1	x	x	x	x			x	x			x	x	x		x
	MPI-M-MPI-ESM-LR r2			x					x					x		
	MPI-M-MPI-ESM-LR r3			x						x				x		
	NCC-NorESM1-M		x	x	x			x		x		x	x	x		x
	IPSL-IPSL-CM5A-LR									x						
	IPSL-IPSL-CM5A-MR		x	x	x			x		x						

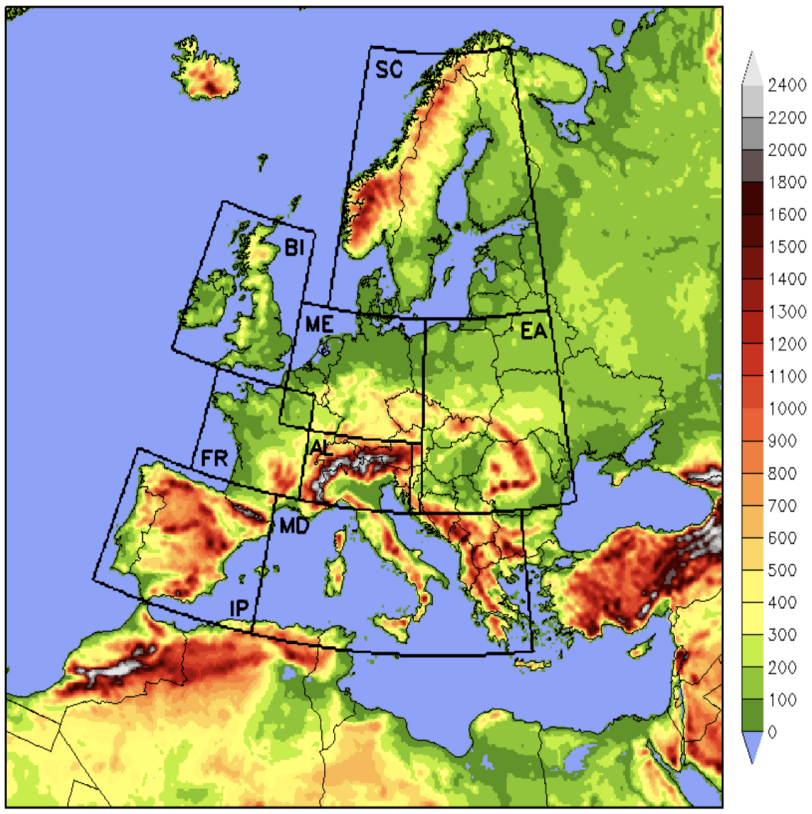

Figure 2.1 Fig. 1 of Kotlarski et al. (2014) showing the EUR-11 computational domain and the PRUDENCE sub-domains, as defined by Christensen and Christensen (2007): British Isles (BI), Iberian Peninsula (IP), France (FR), Mid-Europe (ME), Scandinavia (SC), Alps (AL), Mediterranean (MD), Eastern Europe (EA). The colour represents the orography (m).

2.3 Results

2.3.1 Spatial patterns of the ensemble-median seasonal climate change signals

Figure 2.2 shows the ensemble-median seasonal mean temperature change at 2 m for the full EUR-11 ensemble (including PRINCIPLES) and the previous EUR-11 ensemble (without PRINCIPLES). All simulations agree on a warming in all seasons with the RCP8.5 scenario. The warming is more pronounced in northern Europe in winter and the intermediate seasons, while it is stronger in southern Europe in summer. These results are in agreement with previous studies based on EURO-CORDEX simulations (e.g. Coppola et al. 2021, Evin et al. 2021).

Combining PRINCIPLES simulations with the previous simulations therefore strengthens the conclusion of the EUR-11 ensemble and increases the reliability of the EUR-11 projections, although the full ensemble median is slightly colder than the older ensemble (Fig. 2.3), which dampens the climate change signal. At the northern boundary of the domain, the full ensemble shows a weaker warming. This is particularly strong in winter in the Greenland and Barents Seas (top left panel of Fig. 2.3). This signal, located at the boundary of sea ice cover where the warming signal is strongest, needs to be

investigated to identify whether it is common to all simulations or due to a few RCMs or a particular GCM forcing.

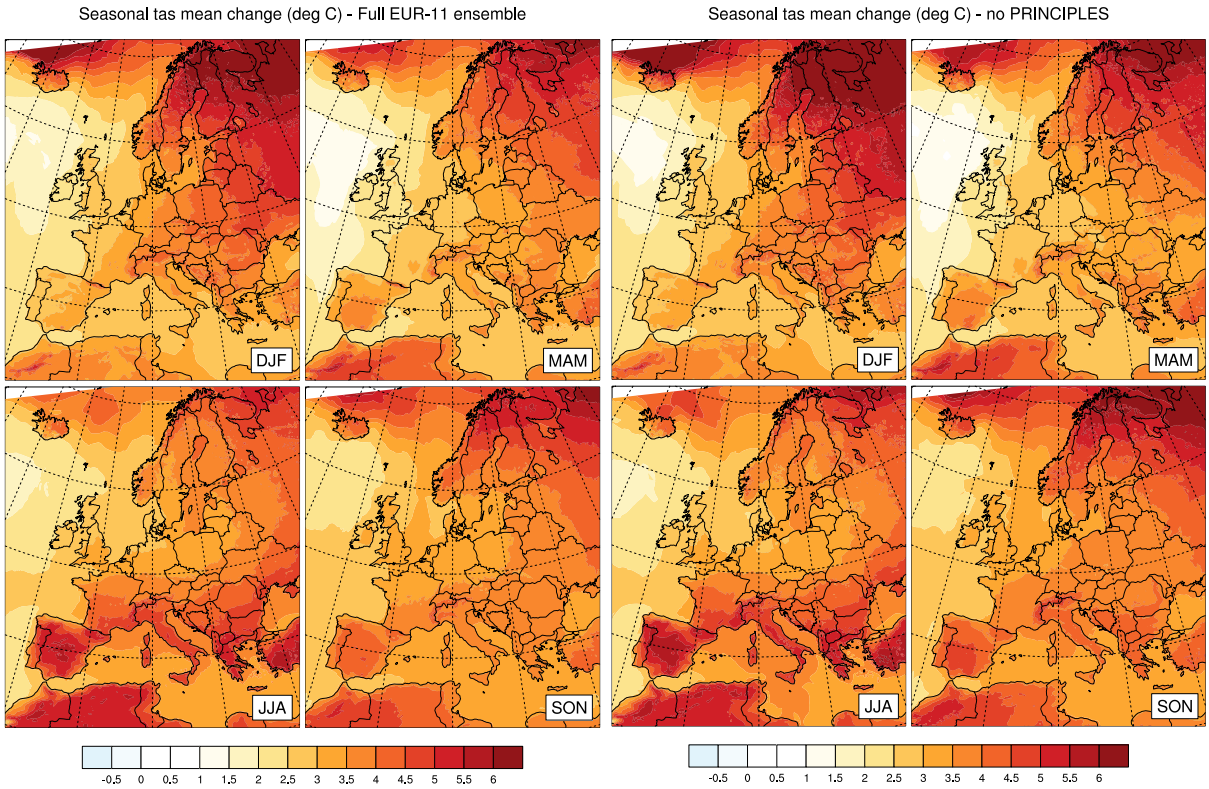

Figure 2.2 Ensemble-median seasonal mean temperature at 2 m change (in degree Celsius) over the EUR-11 domain for the full EUR-11 ensemble including PRINCIPLES (70 members; left panel) and the previous EUR-11 ensemble without PRINCIPLES (24 members; right panel). The change is computed as the difference between the RCP8.5 period (2070-2099) and the historical period (1981-2010). All simulations agree on the sign of changes.

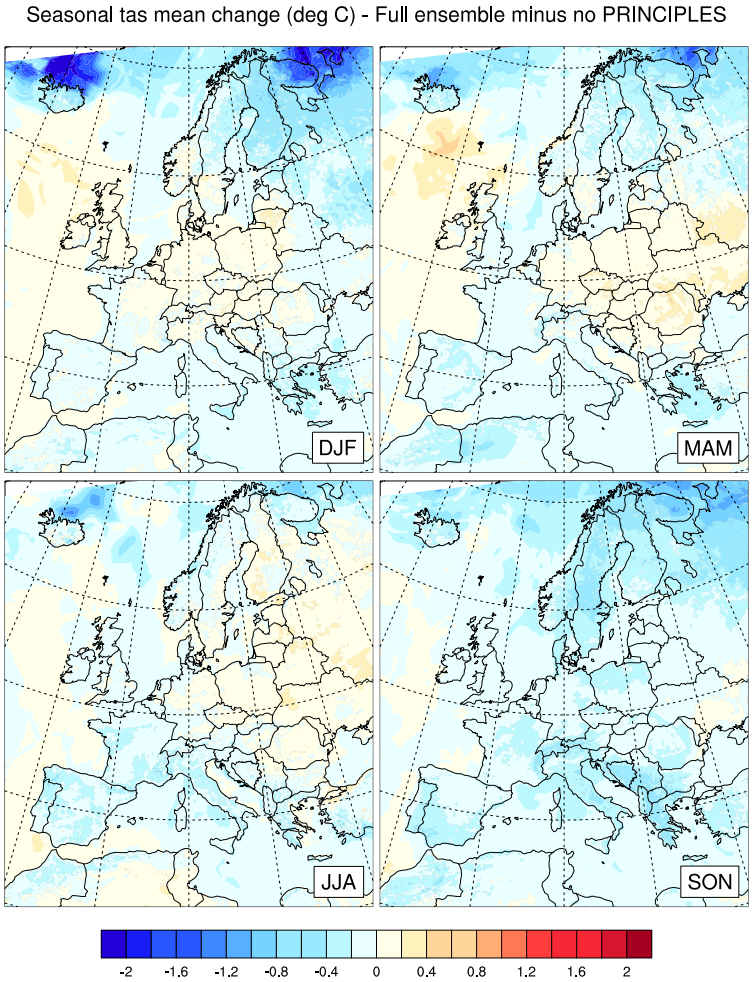

Figure 2.3 Differences in mean temperature at 2 m change (in degree Celsius) between the full EUR-11 ensemble (left panel of Fig. 2.2) and the previous ensemble without PRINCIPLES (right panel of Fig. 2.2).

In terms of changes in mean precipitation (Fig. 2.4) and the 99th percentile of daily precipitation (Fig. 2.5), the spatial patterns between the two ensemble medians are also very similar. Whether the new PRINCIPLES simulations are included or not, the EUR-11 ensemble projects an increase in precipitation mean and extremes in northern Europe and a decrease in southern Europe. These results are in line with previous studies (e.g. Rajczak and Schär 2017, Coppola et al. 2021). However, the large PRINCIPLES ensemble is slightly wetter over southern Europe, which makes the climate change signal in mean and extreme daily precipitation slightly less pronounced compared to the previous EUR-11 ensemble median (Fig. 2.6).

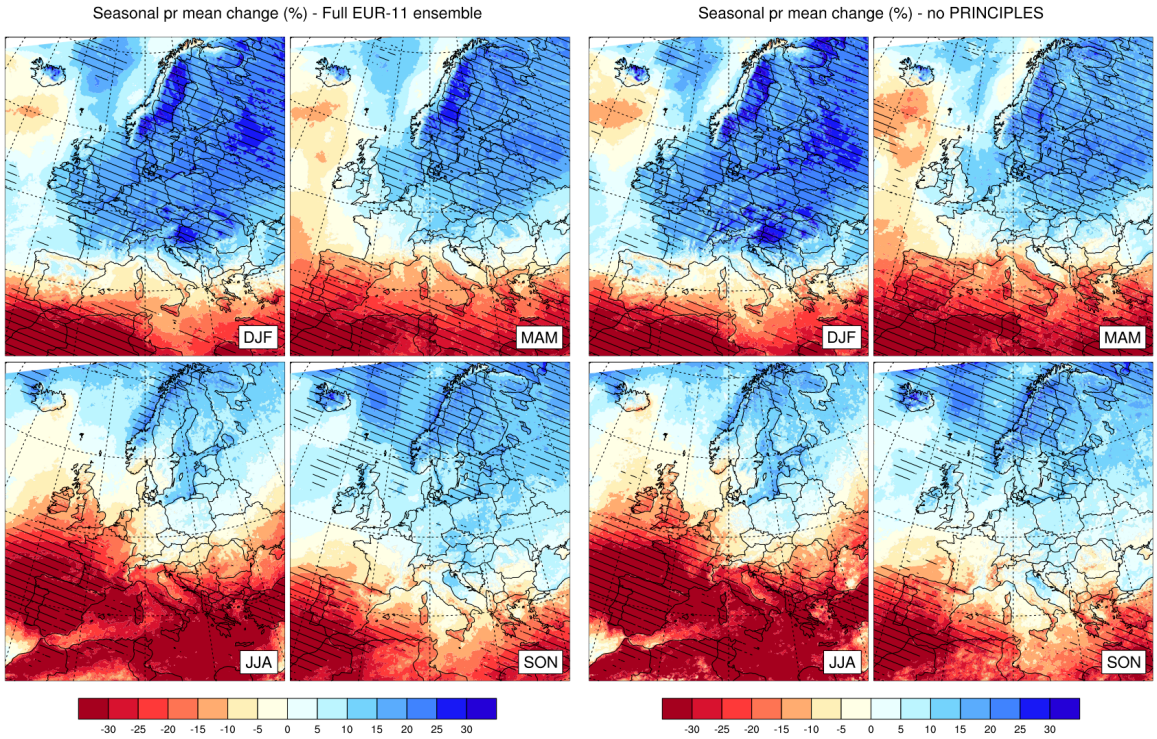

Figure 2.4 Same as Fig. 2.2 for mean precipitation change (in per cent). The change is computed as the relative difference of the RCP8.5 period (2070-2099) with respect to the historical period (1981-2010). The hatching represents areas where 90% of the simulations agree on the sign of changes.

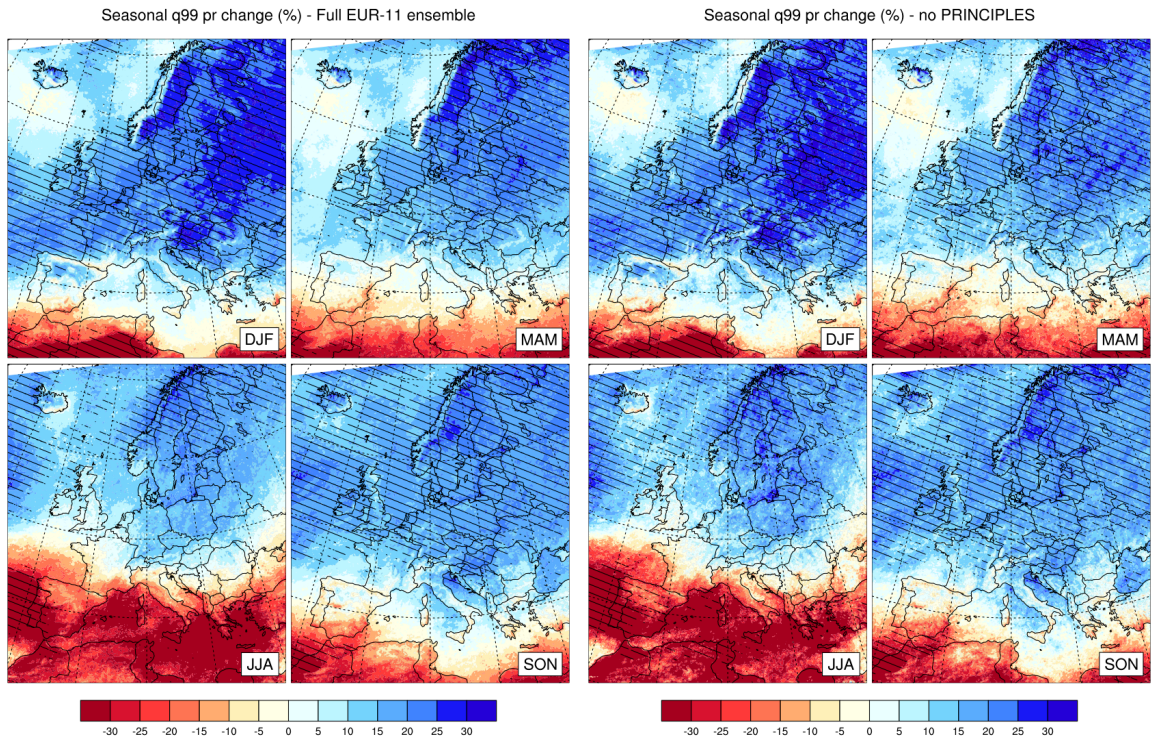

Figure 2.5 Same as Fig. 2.4 for the 99th all-day percentile of daily precipitation changes (in per cent).

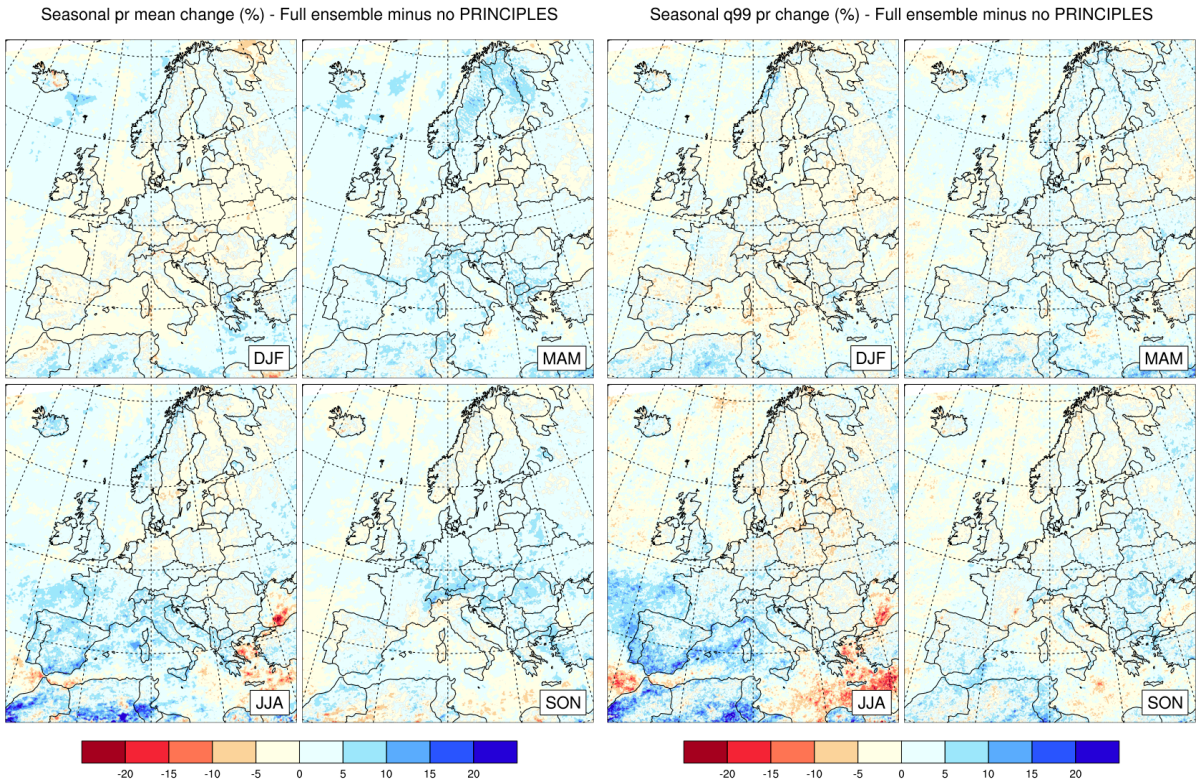

Figure 2.6 Same as Fig. 2.3 for mean precipitation change (in per cent; left panel) and the 99th percentile of daily precipitation change (in per cent; right panel).

2.3.2 Spread of climate change signals

Figure 2.7 shows the seasonal mean precipitation change versus mean change in temperature at 2 m averaged over the PRUDENCE regions for each EUR-11 simulation. Over some regions there is a rather clear relationship between precipitation and temperature. In summer and particularly over southern Europe, the warmer the projection, the drier. This relationship may be explained by the fact that summer warming and drying are not driven by large-scale changes in circulation but mostly by changes in tropospheric lapse-rate caused by thermodynamic processes, which are well represented in most GCMs (Brogli et al. 2019). In other seasons, the results show larger spread. Changes in winter precipitation are not directly linked to local warming, but mostly to changes in large-scale circulation. This is the case for example over the MD region where there is little agreement in projections of winter precipitation, possibly because GCMs tend to not agree on circulation changes (Zappa and Shepherd 2017, Brogli et al. 2019). However, there is some correlation between changes in temperature and changes in precipitation over Scandinavia (SC) and the Iberian Peninsula (IP), likely related to differences in the North Atlantic Oscillation between GCM projections.

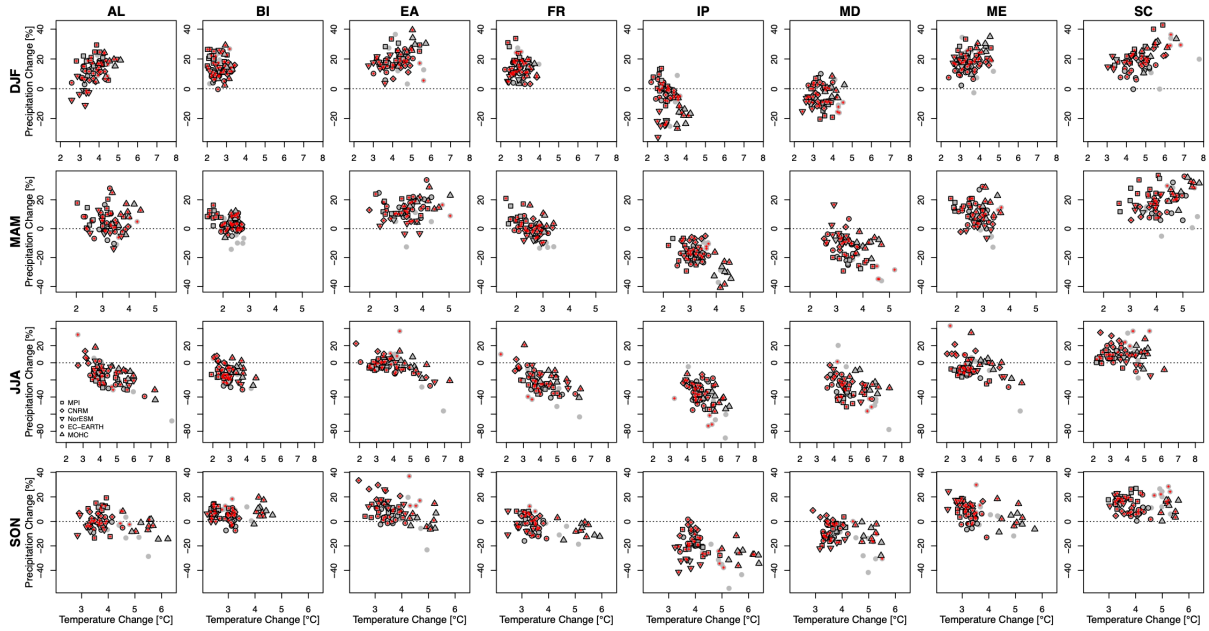

Figure 2.7 Seasonal mean precipitation change (%) versus change in mean temperature at 2 m (degrees Celsius) averaged over the PRUDENCE regions (land points only) for each EUR-11 simulation. Each member is shown with a grey symbol. PRINCIPLES simulations are shown with an additional red symbol. The markers indicate simulations driven by the same GCM (only if there are more than 5 RCMs driven by that GCM; in some cases, this includes several realizations, see Table 2.1): MPI-GCM (square), CNRM-CM5 (diamond), MOHC-HadGEM (upward triangle), NorESM (downward triangle), EC-EARTH (circle). Other points with no boundary are simulations forced with GCMs that were not used by a large number of RCMs. Note that the X- and Y-axis scales are fixed across regions for each season.

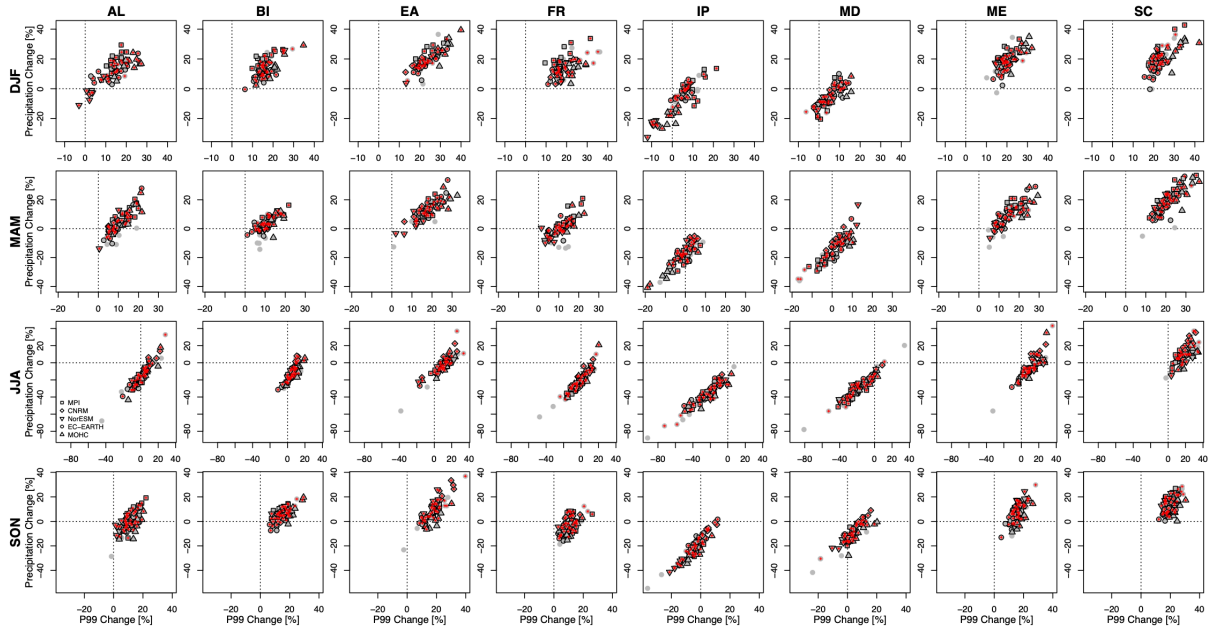

Figure 2.8 Same as Fig. 2.7 for seasonal mean precipitation change (%) versus the 99th percentile of all-day precipitation change (%) averaged over the PRUDENCE regions (land points only) for each EUR-11 simulation.

The relationship between mean precipitation and extreme precipitation (represented by the 99th percentile of daily precipitation) is shown in Fig. 2.8. As expected, all GCM-RCM simulations that project a smaller (larger) change in mean precipitation also project a smaller (larger) change in extreme precipitation over all regions and in all seasons. The spread of the relationship is larger in some regions (e.g. AL, BI, FR, ME, SC) and mostly in DJF and SON, while the relationship is particularly clear in JJA in all regions.

Figures 2.7 and 2.8 also give an indication of the impact of including the large PRINCIPLES ensemble on the spread of the projected changes. Inclusion of PRINCIPLES tends to increase the spread of the signal although not systematically in all seasons and regions. Most PRINCIPLES simulations (red symbols in Fig. 2.7) stand among the previous EUR-11 simulations (grey symbols). There are, however, some clear signals depending on the GCM forcings. For example, RCMs forced with the HadGEM2-ES GCM (shown with the upward triangle) commonly stand on the warmer side of the distribution. This result is consistent with Evin et al. (2021).

Similarly, including PRINCIPLES simulations into the EUR-11 ensemble tends to slightly increase the spread of extreme daily precipitation change in most seasons and over most regions, particularly in topographically diverse and coastal regions (AL, BI, IP, MD, ME; Fig. 2.8). Again, some signals appear to depend on the GCM forcings. The RCMs forced with the NorESM GCM tend to simulate smaller changes or stronger decrease in mean and extreme precipitation (downward triangle in Fig. 2.8). This is the case in almost all regions in winter and in the Alps (AL) in all seasons but summer. We can also identify an outlier in the older ensemble in almost all regions in JJA and SON: CLMcom-CCLM4-8-17_CCCma-CanESM2_r1i1p1 (bottom right grey circle in Fig. 2.7 and bottom left grey circle in Fig. 2.8). This simulation also stands out as being a lot warmer and drier than the ensemble in the ANOVA analyses (Fig. 1.4 and 1.9). The CanESM2 GCM was only used to force two RCMs so it is difficult to determine the robustness of this response. Such outliers, however, may not be wrong. They offer an opportunity to better understand the effect of driving conditions on the European climate change signal. The RCM projections driven by the MPI GCM show larger spread (Fig. 2.8). MPI includes more realizations (as does EC-EARTH; Table 2.1). Preliminary analyses show that the results tend to group around the GCM realization or around the RCM depending on regions and seasons (not shown). Internal variability could therefore play a role in the spread of the projections (more analyses will be performed later).

To quantify the ensembles spread more clearly, box-and-whisker plots are drawn for each region and season for mean temperature (Fig. 2.9), mean precipitation (left panel of Fig. 2.10) and the 99th percentile of daily precipitation (right panel of Fig. 2.10). We see that median changes in mean temperature are generally smaller in the full ensemble (when adding PRINCIPLES; thick black lines in Fig. 2.9) than in the previous ensemble with no PRINCIPLES simulations (thick blue lines in Fig. 2.9). This is common for all regions and seasons, and confirms the results shown in Fig. 2.2 and 2.3. The interquartile ranges (black boxes), as well as the spread (black whiskers) tend to be slightly larger in the full ensemble in DJF in all regions, particularly on the lower and hence colder side of the

distribution. In summer and autumn, the interquartile range is smaller in the full ensemble in all regions (except in the Scandinavian region SC in SON), which indicates that projections are closer to the full ensemble median. The spread of the full ensemble is either larger or similar to the previous ensemble spread. In SON, there are also more outliers, so more extreme projections, in the full ensemble. The results are mixed in spring.

In terms of mean precipitation (left panels of Fig. 2.10), the two ensemble medians tend to be similar in most seasons and regions, although the full ensemble tends to be slightly wetter (Fig. 2.6). The interquartile range also tends to be similar between the two ensembles, although slightly smaller in the full ensemble in most regions but in the Alps (AL) in spring. However, the spread is larger in the full ensemble in almost all regions and seasons but in France (FR) in spring (black whiskers in left panel of Fig. 2.10). These results imply that adding PRINCIPLES simulations to the previous ensemble does not change the main conclusions of the EUR-11 ensemble, as most of the simulations are concentrated within the interquartile range, but tends to increase the spread in projections of mean precipitation. This could be related to the choice of the GCM (e.g. HadGEM2-ES or CNRM-CM5) that forces the RCMs towards one side of the distribution (Fig. 2.7).

In terms of extreme precipitation (right panels of Fig. 2.10), the results are similar to mean precipitation. However, there are more outliers in the previous ensemble (blue points outside the whiskers) in summer. The most extreme one is identified as CLMcom-CCLM4-8-17_CCCma-CanESM2_r1i1p1 with extreme precipitation changes up to -80% (blue circle in JJA right panel of Fig. 2.10).

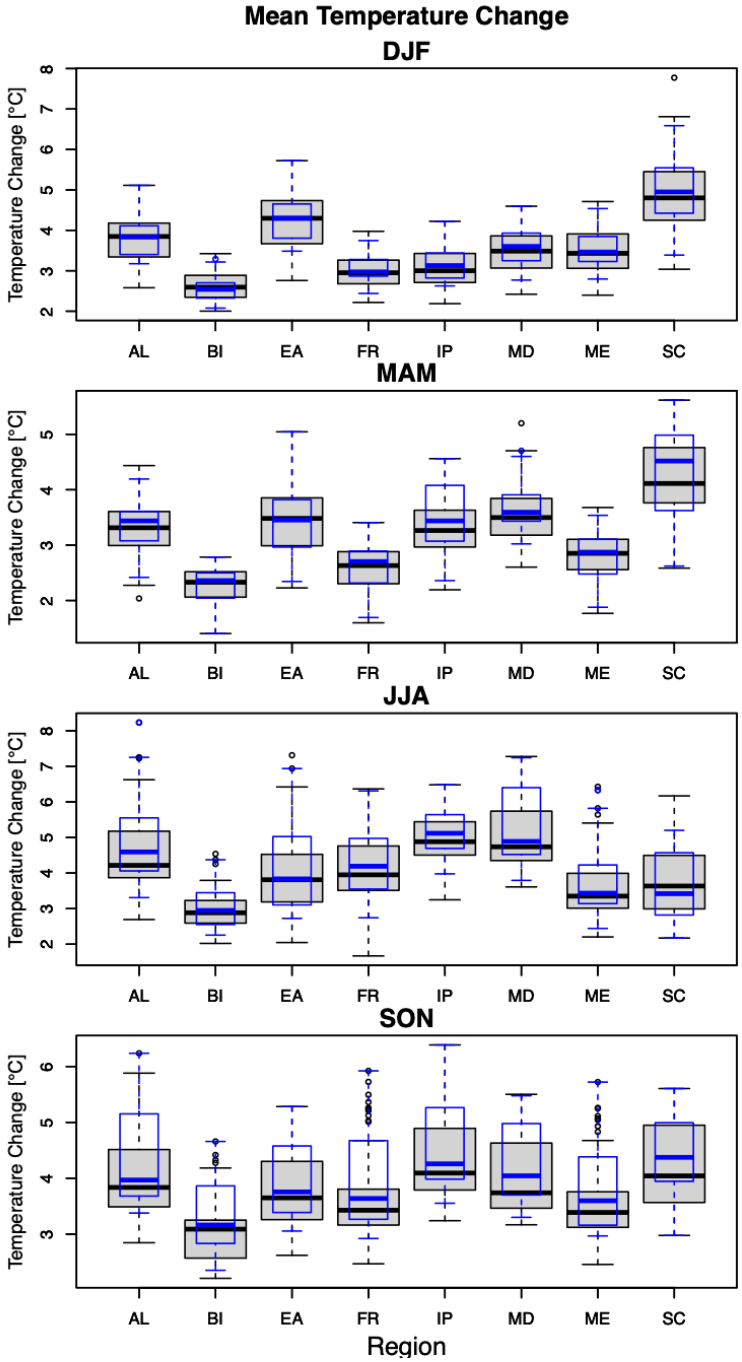

Figure 2.9 Box-and-whisker plots of changes in mean temperature (in degree Celsius) over each European sub-region as defined in Fig. 2.1. Each box represents the interquartile range (IQR) with the 25th percentile at the lower boundary and the 75th percentile at the upper boundary. Within each box, the thick horizontal line represents the ensemble median. From above the upper (below the lower) boundary of the box, a distance of 1.5 times the interquartile range is computed and a whisker is drawn up to the largest (lowest) value that falls within this distance (drawn at the 75th percentile + 1.5 × IQR and at the 25th percentile - 1.5 × IQR). Values outside the whiskers are considered outliers (indicated by dots). The black colour represents the full ensemble; the blue colour represents the previous ensemble with no PRINCIPLES simulations.

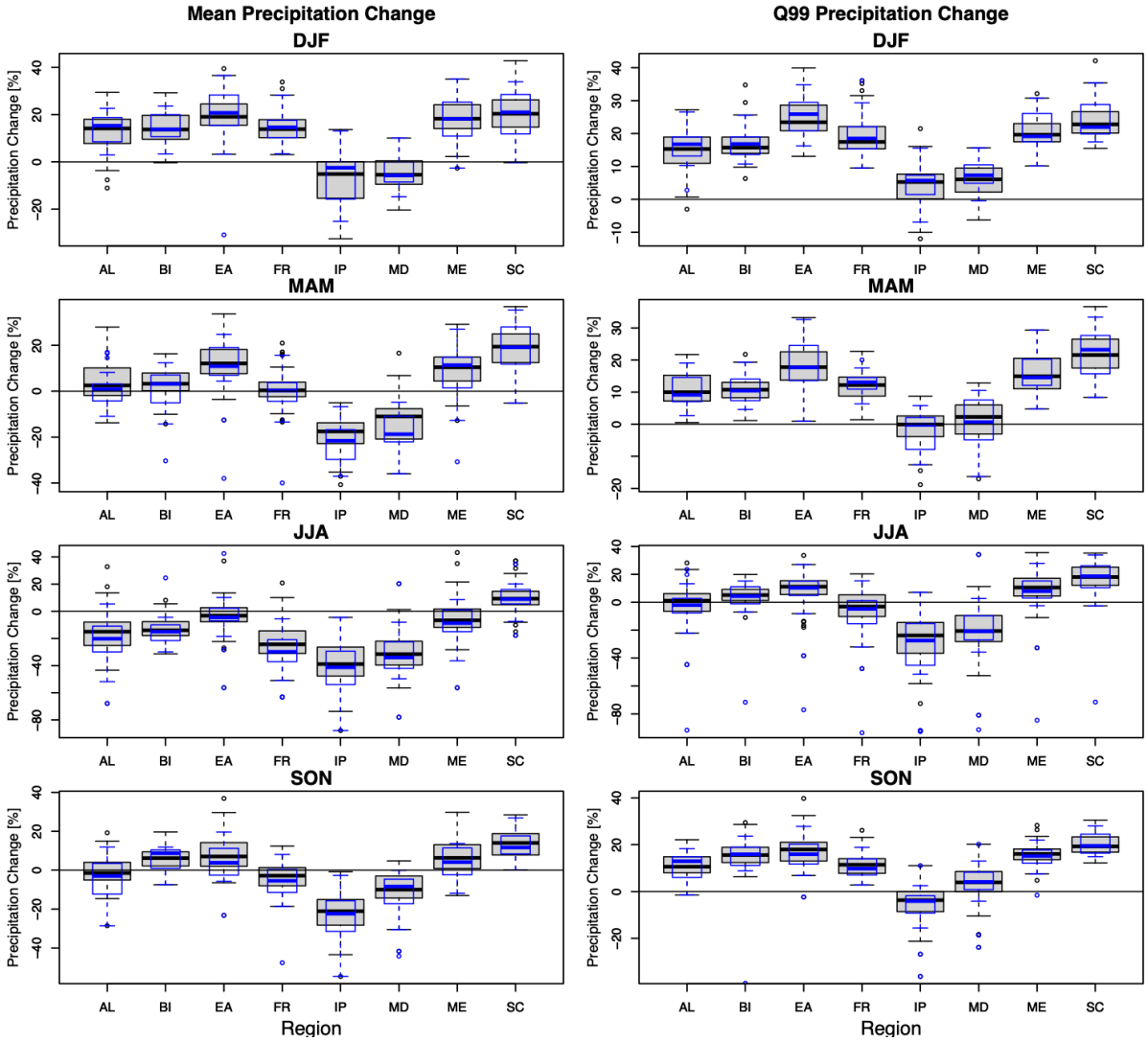

Figure 2.10 Same as Fig. 2.9 for changes in mean precipitation (in per cent; left panel) and the 99th percentile of all-day precipitation (in per cent; right panel).

2.4 Conclusion and future work

This study makes use of the full EUR-11 ensemble now available at ESGF and evaluates the impact of the additional PRINCIPLES simulations (bringing a total of 70 EUR-11 simulations so far) compared to the simulations performed before PRINCIPLES (24 simulations).

The PRINCIPLES simulations give confidence to the previous results of the EUR-11 ensemble. Our results show that adding PRINCIPLES to the previous EUR-11 ensemble does not impact the ensemble-median largely, although PRINCIPLES projections tend to be somewhat colder and wetter, particularly in southern Europe, which slightly mitigates the climate change signal. For some regions, the differences between the previous EUR-11 ensemble and the full ensemble including PRINCIPLES clearly depend on the GCM forcings. The ensemble interquartile range is generally similar or even smaller in the full ensemble than the previous ensemble (but slightly larger for winter mean temperature), which

indicates that most additional projections tend to group around others and therefore are closer to the ensemble median. However, the spread of the full ensemble tends to be slightly larger, mainly due to the addition of one or two GCM forcings: the MOHC-HadGEM2-ES GCM, which tends to force the RCMs on a warmer side in most regions and seasons, and the CNRM-CERFACS-CNRM-CM5 GCM, which tends to be colder and wetter in summer. There are also some intermodel variabilities for each GCM forcing due to differences in RCMs. This is particularly true in summer (Fig. 2.7). These GCM-RCM outliers that project more extreme changes give potentials to better understand the drivers of such signals, whether they are due to GCM driving conditions or to RCM features. This opportunity would not be possible without such a large ensemble.

According to these preliminary results, we agree with Vautard et al. (2020) and Coppola et al. (2021) that the large EUR-11 GCM-RCM matrix strengthens our confidence in the climate change signal projected by the current model generation of 12 km resolution RCMs. Additional EUR-11 simulations may not change the main results of the current ensemble largely regarding mean changes in the fields studied here (temperature at 2 m and precipitation). Instead, our results show that the choice of the GCM is essential. It may therefore be necessary to choose a few supplementary GCMs that cover a wide range of climate sensitivity, for example low, medium and high climate sensitivity, as well as GCMs that cover a wide range of climate change response over Europe.

This study is currently ongoing and only one scenario has been used. More analyses, including more complex analyses such as extreme value analyses, will be performed to make full use of the complete EUR-11 RCP-GCM-RCM matrix.

3. Conclusion

The EUR-11 ensemble analysed in this report, and publicly available at ESGF and the Copernicus Climate Data Store (CDS), is the largest ensemble of regional climate model projections ever produced for Europe. It offers an unprecedented opportunity for studying the accuracy and trustworthiness of climate change projections. Through two independent studies, we find that the EUR-11 ensemble projections are similar to previous studies based on smaller ensembles (Rajczak and Schär 2017, Coppola et al. 2021) or emulated ones (Christensen and Kjellström 2021). These findings give confidence to the EUR-11 projections of climate change over Europe, at least for the temperature, precipitation and wind fields studied here.

The two above studies also show that GCMs play a large role for the RCM projections, particularly in winter for temperature and precipitation, resulting in an increase in the spread of the projections when more GCMs are included into an ensemble. This strong sensitivity to the GCMs and their representation of the large-scale circulation has strong implications for GCM-RCM matrix design and we note that future ensembles could be built with a larger range of GCMs, without the need to fill the GCMxRCM matrix with the RCMs entirely. However, keeping a minimum degree of filling is still required, as shown by the ANOVA analyses. In summer particularly, the projections are less sensitive to the GCMs' forcings and in this case keeping a diversity of RCMs is necessary. The same argumentation applies to fields with a large internal variability and to extreme events.

The general strategy in the PRINCIPLES project has been to establish filled sub-matrices of the 3-dimensional RCPxGCMxRCM matrix. Such sub-matrices like the one studied in Christensen and Kjellström (2020, 2021) are prerequisites for the ANOVA-based matrix completion and for estimates of the associated errors in it calculated from successive degradation of a full matrix (Christensen and Kjellström, 2021). As such, this strategy has proven very useful. Future matrix-filling strategies should probably be changed as mentioned above towards more GCMs being downscaled by several, but not necessarily all, available RCMs.

There is still a need for a thorough analysis of the RCP aspect, i.e., how much added value an almost filled matrix for one emission scenario gives to more sparsely filled matrices for other emission scenarios. This is an obvious extension of the research described presently and is planned to be pursued in the near future. Another natural extension would be around expanding the analysis to other variables and modes of variability including extremes on different scales. This would be especially important for some impact studies and as guidance for users of the PRINCIPLES climate projections provided by the C3S.

4. References

Bentsen M, Bethke I, Debernard JB, Iversen T, Kirkevåg A, Seland Ø, Drange H, Roelandt C, Seierstad IA, Hoose C, Kristjánsson JE (2013) The Norwegian Earth System Model, NorESM1-M—Part 1: description and basic evaluation of the physical climate. *Geosci Model Dev* **6**, 687–720, https://doi.org/10.5194/gmd-6-687-2013

Brogli R, Kröner N, Sørland SL and Schär C (2019) Causes of Future Mediterranean Precipitation Decline Depend on the Season. *Environ Res Lett* **14**, 114017, https://doi.org/10.1088/1748-9326/ab4438

Christensen JH and Christensen OB (2007) A summary of the PRUDENCE model projections of changes in European climate by the end of this century. *Climatic Change* **81**, 7–30, https://doi.org/10.1007/s10584-006-9210-7

Christensen OB, Drews M, Christensen JH, Dethloff K, Ketelsen K, Hebestadt I and Rinke A (2007) The HIRHAM Regional Climate Model. Version 5 (beta). Danish Climate Centre, Danish Meteorological Institute. Denmark. Danish Meteorological Institute. Technical Report, No. 06-17

Christensen OB, and Kjellström E (2020) Partitioning uncertainty components of mean climate and climate change in a large ensemble of European regional climate model projections. *Clim Dyn* https://doi.org/10.1007/s00382-020-05229-y

Christensen OB, and Kjellström E (2021) Filling the matrix: An ANOVA-based method to emulate regional climate model simulations for equally-weighted properties of ensembles of opportunity. Submitted to *Clim Dyn* Preprint at https://assets.researchsquare.com/files/rs-366374/v1_stamped.pdf

Chylek P, Li J, Dubey MK, Wang M and Lesins G (2011) Observed and model simulated 20th century Arctic temperature variability: Canadian Earth System Model CanESM2. *Atmos Chem Phys Discuss* **11**, 22 893–22 907, https://doi.org/10.5194/acpd-11-22893-2011

CNRM (2018). Issue in some CNRM-CM5 files and implications for CMIP5 and CORDEX users, http://www.umr-cnrm.fr/cmip5/IMG/pdf/communication-issue-files_cnrm-cm5_historical_6hlev_en.pdf

Collins WJ, Bellouin N, Doutriaux-Boucher M, Gedney N, Halloran P, Hinton T, Hughes J, Jones CD, Joshi M, Liddicoat S, Martin G, O'Connor F, Rae J, Senior C, Sitch S, Totterdell I, Wiltshire A, Woodward S (2011) Development and evaluation of an Earth-System model – HadGEM2. *Geosci Model Dev* **4**, 1051–1075, https://doi.org/10.5194/gmd-4-1051-2011

Coppola E, Nogherotto R, Ciarlò JM, Giorgi F, van Meijgaard E, Iles C, Kadygrov N, Corre L, Sandstad M, Somot S, Nabat P, Vautard R, Levavasseur G, Schwingshackl C, Sillmann J, Kjellström E, Nikulin G,

Aalbers E, Lenderink G, Christensen OB, Boberg F, Sørland SL, Demory M-E, Bülow K, Teichmann C (2021) Assessment of the European climate projections as simulated by the large EURO-CORDEX regional climate model ensemble, *J Geophys Res Atmos* **126**, e2019JD032356, https://doi.org/10.1029/2019JD032356

Dufresne J-L and Coauthors (2013) Climate change projections using the IPSL-CM5 Earth System Model: FromCMIP3 to CMIP5. *Clim Dyn* **40**, 2123–2165, https://doi.org/10.1007/s00382-012-1636-1

Evin G, Somot S and Hingray B (2021) Balanced estimate and uncertainty assessment of European climate change using the large EURO-CORDEX regional climate model ensemble, *Earth Syst Dynam Discuss* [preprint], https://doi.org/10.5194/esd-2021-8

Giorgetta MA et al. (2013) Climate and carbon cycle changes from 1850 to 2100 in MPI-ESM simulations for the Coupled Model Intercomparison Project phase 5. *J Adv Model Earth Syst* **5**, 572–597, https://doi.org/10.1002/jame.20038

Giorgi F, Coppola E, Solmon F, Mariotti L, Sylla MB, Bi X, Elguindi N, Diro GT, Nair V, Giuliani G, Turuncoglu UU, Cozzini S, Güttler I, O'Brien TA, Tawfik AB, Shalaby A, Zakey AS, Steiner AL, Stordal F, Sloan LC, Brankovic C (2012) RegCM4: model description and preliminary tests over multiple CORDEX domains. *Clim Res* **52**(1), 7–29, https://doi.org/10.3354/cr01018

Hazeleger W, Wang X, Severijns C, Ştefănescu S, Bintanja R, Sterl A, Wyser K, Semmler T, Yang S van den Hurk B, van Noije T, van der Linden E, van der Wiel K (2012) EC-Earth V2.2: description and validation of a new seamless earth system prediction model. *Clim Dyn* **39**, 2611, https://doi.org/10.1007/s00382-011-1228-5

Jacob D, Elizalde A, Haensler A, Hagemann S, Kumar P, Podzun R, Rechid D, Remedio AR, Saeed F, Sieck K, Teichmann C, Wilhelm C (2012) Assessing the transferability of the regional climate model REMO to different coordinated regional climate downscaling experiment (CORDEX) regions. *Atmosphere* **3**, 181–199, https://doi.org/10.3390/atmos3010181

Kotlarski S, Keuler K, Christensen OB, Colette A, Déqué M, Gobiet A, Goergen K, Jacob D, Lüthi D, van Meijgaard E, Nikulin G, Schär C, Teichmann C, Vautard R, Warrach-Sagi K and Wulfmeyer V (2014) Regional climate modeling on European scales: a joint standard evaluation of the EURO-CORDEX RCM ensemble, *Geosci Model Dev* **7**, 1297–1333, https://doi.org/10.5194/gmd-7-1297-2014

Leutwyler D, Lüthi D, Ban N, Fuhrer O, Schär C (2017). Evaluation of the Convection-Resolving Climate Modeling Approach on Continental Scales. *J Geophys Res Atmos* **122**, 5237-5258, http://dx.doi.org/10.1002/2016JD026013

Nabat P, Somot S, Cassou C, Mallet M, Michou M, Bouniol D, Decharme B, Drugé T, Roehrig R and Saint-Martin D (2020) Modulation of radiative aerosols effects by atmospheric circulation over the Euro-Mediterranean region, *Atmos Chem Phys* **20**, 8315–8349, https://doi.org/10.5194/acp-20-8315-2020

Raddatz T and Coauthors (2007) Will the tropical land biosphere dominate the climate–carbon cycle feedback during the twenty-first century? *Clim Dyn* **29**, 565–574, https://doi.org/10.1007/s00382-007-0247-8

Rajczak J and Schär C (2017) Projections of future precipitation extremes over Europe: A multimodel assessment of climate simulations. *J Geophys Res Atm* **122**, 10 773–10 800, https://doi.org/10.1002/2017JD027176

Rockel B, Will A, Hense A (2008) The Regional Climate Model COSMO-CLM (CCLM). *Meteorol Z* **17**, 347–348 https://doi.org/10.1127/0941-2948/2008/0309

Samuelsson P, Jones C, Willén U, Ullerstig A, Gollvik S, Hansson U, Jansson C, Kjellström E, Nikulin G, Wyser K (2011) The Rossby Centre Regional Climate Model RCA3: model description and performance. *Tellus* A **63**, 4–23, https://doi.org/10.1111/j.1600-0870.2010.00478.x

Skamarock WC, Klemp JB (2008) A time-split nonhydrostatic atmospheric model for weather research and forecasting applications. *J Comput Phys* **227**(7), 3465–3485, https://doi.org/10.1016/j.jcp.2007.01.037

Sørland S, Lüthi D, Schär C, Kjellström E (2018) Bias patterns and climate change signals in GCM–RCM model chains. *Environ Res Lett* **13**, 074017, https://doi.org/10.1088/1748-9326/aacc77

van Meijgaard E, van Ulft LH, van den Berg WJ, Bosveld FC, van den Hurk BJJM, Lenderink G, Siebesma AP (2008), The KNMI regional atmospheric climate model RACMO version 2.1. KNMI Tech. Rep. TR-302, 43 pp

van Meijgaard E, van Ulft LH, Lenderink G, de Roode SR, Wipfler L, Boers R and Timmermans RMA (2012) Refinement and application of a regional atmospheric model for climate scenario calculations of Western Europe, Climate changes Spatial Planning publication: KvR 054/12, the Programme Office Climate changes Spatial Planning, Nieuwegein, the Netherlands, ISBN/EAN 978-90-8815-046-3, 44 pp. http://climexp.knmi.nl/publications/FinalReport_KvR-CS06.pdf

Vautard R, Kadygrov N, Iles C, Boberg F, Buonomo E, Coppola E, Bülow K, Corre L, van Meijgaard E, Nogherotto R, Sandstad M, Schwingshackl C, Somot S, Aalbers E, Christensen OB, Ciarlò JM, Demory M-E, Giorgi F, Jacob D, Jones RG, Keuler K, Kjellström E, Lenderink G, Levavasseur G, Nikulin G, Sillmann J, Solidoro C, Sørland SL, Steger C, Teichmann C, Warrach-Sagi K and Wulfmeyer V (2020) Evaluation of the large EURO-CORDEX regional climate model ensemble. *J Geophys Res Atmos* **125**, e2019JD032344, https://doi.org/10.1029/2019JD032344

Voldoire A, Sanchez-Gomez E, Salas y Mélia D et al. (2013) The CNRM-CM5.1 global climate model: description and basic evaluation. *Clim Dyn* **40**, 2091. https://doi.org/10.1007/s00382-011-1259-y

Walters D, Baran A, Boutle I, Brooks M, Earnshaw P, Edwards J, Furtado K, Hill P, Lock A, Manners J, Morcrette C, Mulcahy J, Sanchez C, Smith C, Stratton R, Tennant W, Tomassini L, Van Weverberg K, Vosper S, Willett M, Browse J, Bushell A, Dalvi M, Essery R, Gedney N, Hardiman S, Johnson B, Johnson C, Jones A, Mann G, Milton S, Rumbold H, Sellar A, Ujiie M, Whitall M, Williams K and Zerroukat M (2017) The Met Office Unified Model Global Atmosphere 7.0/7.1 and JULES Global Land 7.0 configurations, *Geosci Model Dev* **12**, 1909–1963, 2019, https://doi.org/10.5194/gmd-12-1909-2019

Watanabe M and Coauthors (2010) Improved climate simulation by MIROC5: Mean states, variability, and climate sensitivity. *J Clim* **23**, 6312–6335, https://doi.org/10.1175/2010JCLI3679.1

Zappa G and Shepherd TG (2017) Storylines of Atmospheric Circulation Change for European Regional Climate Impact Assessment. *J Clim* **30**, 16, 6561-6577, https://doi.org/10.1175/JCLI-D-16-0807.1

Copernicus Climate Change Service

ECMWF - Shinfield Park, Reading RG2 9AX, UK

Contact: info@copernicus-climate.eu

climate.copernicus.eu copernicus.eu ecmwf.int